Award Number G12AP20069

Plio-Quaternary reactivation of Miocene faults by the Newport-Inglewood-Rose Canyon-San Mateo-Carlsbad-Descanso-Coronado Bank fault system: Newport Beach to San Diego, California

Authors: **Christopher C. Sorlien** (P.I.), **Jonathan T. Bennett, Marie-Helene Cormier**

Report date August 10, 2013.

Sorlien: Earth Research Institute
University of California, Santa Barbara
email: sorlien@eri.ucsb.edu
Home office phone in Rhode Island: 401-560-0368

Bennett: Department of Geology, University of Missouri
Now at Fugro, Houston, Texas

Cormier: Department of Geology, University of Missouri
milenecormier@gmail.com

Term of award: May 1, 2012 – April 30, 2013

"Research supported by the U.S. Geological Survey (USGS), Department of the Interior, under USGS award number G12AP20069. The views and conclusions contained in this document are those of the authors and should not be interpreted as necessarily representing the official policies, either expressed or implied, of the U.S. Government."

ABSTRACT

Identification of the problem and implications

The near offshore between Santa Monica and San Diego includes right-lateral faults with several mm/yr. combined slip rates. Regional-scale low-angle Miocene normal faults are imaged that dip beneath the mainland coast. Recent publications on the offshore shelf, slope, and adjoining basins between Long Beach and San Diego strongly disagree on fault geometry, continuity, and kinematics, as well as stratigraphy. The extent of contractional folding and its relation to regional low-angle faults affects the probability of major thrust earthquakes vs. the <M6 historic thrust quakes. Obviously a thrust rupture extending 200 km along the linked Santa Monica Bay-Catalina Island detachment-30 Mile Bank "thrust", or a 100 km thrust rupture on the Oceanside "thrust", both extending farther into Mexican waters, would have strong ground motion and tsunami consequences. Alternatively, thrusting focused in the north, or strike-slip faulting with thrusting only on restraining segments, could still produce damaging earthquakes, but the spatial extent and duration of strong ground motion, and the extent and size of tsunamis, would be very different.

Summary of Approach

We analyzed several thousand kilometers of deep-penetration industry multi-channel seismic reflection data (MCS), high resolution U.S. Geological Survey MCS profiles, bathymetry, and published and Bureau of Ocean Energy Management interpretations of well and core data. Interpretations of faults and Plio-Quaternary stratigraphic horizons through all the MCS data were gridded and depth-converted. The known 3D fault attitude and structural relief of a 1.95 Ma horizon were inputs to trigonometric displacement modeling using ranges of directions and magnitudes of the hanging-wall above a fault.

Results

The San Mateo-Carlsbad fault forms a downward-converging transpressional "flower structure" geometry with the right-lateral Newport-Inglewood fault. South of 33 degrees N, several left-stepping en-echelon strands of the Coronado Bank fault zone form a transtensional (negative) flower structure geometry with the Descanso fault in Miocene through Quaternary strata. There is an ~18 km-wide right stepover between the northern and southern flower structures. The trigonometric modeling indicates between 0.6 and 1.0 km of post-~1.95 Ma pure right-lateral displacement at the northern bend of the stepover. Similar patterns of deformation of four post-780 ka horizons suggest that slow right-lateral slip continued through late Quaternary time. This stepover marks a boundary between regional Quaternary transpression in the north and transtension in the south.

Folding above regional low-angle Miocene normal faults suggests Quaternary thrust-reactivation. No significant Quaternary contractional folding is imaged on MCS data south of the right-releasing stepover, between 30 km northwest of San Diego and the offshore Mexican border. Thus, either there is little thrust hazard south of latitude 33°, or thrusting is too young and/or too slow to build significant structure. The Palos Verdes anticlinorium overrides the low-angle faults north of latitude 33.5°, but the upper, southwest parts of these faults have not been significantly thrust-reactivated, except locally associated with bends in right-lateral faults.

1: **Introduction**

Prominent continental transform fault systems, such as the San Andreas [e.g., *Hill and Dibblee*, 1953], the North Anatolian in northwest Turkey [e.g., *Sengor* et al., 2005; *Sorlien et al.*, 2012], and the Marlborough in New Zealand [e.g., *Roberts,* 1995], are characterized by broad zones of distributed faulting. Faults along the southern California margin and in continental crust elsewhere in the world commonly reactivate older faults from previous tectonic regimes. Reactivated faults may be unfavorably oriented for the current strain. Moderately-dipping strike-slip faults with displacements from a few km to over 100 km have been documented in California. These faults include the large-displacement San Gregorio fault offshore of the city of Santa Cruz [*Langenheim et al.*, 2012], the southern San Andreas fault [*Nicholson*, 1996; *Fuis et al., 2012*, and the Santa Monica-Dume fault offshore Malibu [*Sorlien et al.*, 2006]. We document the geometry of many faults between Santa Monica and San Diego within 30 to 40 km of the modern coast. We also model kinematics of a fault with low Quaternary displacement within a larger system of nearshore faults between Long Beach and San Diego. This fault, the San Mateo-Carlsbad, is strike-slip in its moderately-dipping segment. It reactivates a Miocene (oblique) normal fault in a region of major Miocene extension [e.g., *Crouch and Suppe*, 1993].

The southern California margin and current offshore Continental Borderland experienced up to hundreds of kilometers of early and middle Miocene extension [e.g., *Crouch and Suppe*, 1993]. This extension was accommodated on regional scale low-angle (oblique) normal faults, as well as on moderately-dipping faults [e.g., *Bohannon and Geist*, 1998]. Gently-dipping NNE to ENE-dipping faults have been documented within 30 km of the present coast between Santa Monica and San Diego [*Nicholson et al.*, 1993; *Rivero et al.*, 2000; *Sorlien et al.*, 2013]. The Miocene motion of the Pacific Plate away from the North American Plate [e.g., *Atwater and Stock*, 1998] facilitated the clockwise vertical axis rotation of the western Transverse Ranges [e.g., *Kamerling and Luyendyk*, 1985]. Gradual late Miocene plate motion changes and the jump of the Pacific-North American plate boundary to the Gulf of California initiated the southern San Andreas fault with its restraining Mojave segment [*Crowell*, 1979; *Atwater and Stock*, 1998; *Nicholson et al.*, 1994; *Wilson et al.*, 2005]. The resulting Plio-Quaternary transpression resulted in thrust faulting and basin inversion [*Wright*, 1991; *Yeats and Beall*, 1991; *Seeber and Sorlien*, 2000]. Thrust earthquakes lead to recognition of blind thrust faults around Los Angeles basin [*Davis et al.*, 1989; *Shaw and Suppe*, 1996; Shaw and Shearer, 1999; *Rivero et al.*, 2000].

Faults in the study area generally strike northwest, and Quaternary slip on them is right-lateral, thrust, or oblique (Figs 1, 2) [*Legg*, 1991; *Nicholson et al.*, 1993; *Ryan et al.*, 2009; *Rivero and Shaw*, 2011; *Sorlien et al.*, 2010]. Recently published fault maps have major disagreements on fault continuity, location, or even existence [*Plesch et al.*, 2007; *Ryan et al.*, 2009; *Sorlien et al.*, 2010; *Jennings et al.*, 2010; *Rivero and Shaw*, 2011]. There is disagreement about which faults are right-lateral, which are reverse, and where Miocene faults have been reactivated and are currently hazardous.

Several large faults within 30 km of the coast have been proposed to be thrust faults [*Rivero et al*, 2000; *Rivero and Shaw*, 2011; *Sorlien et al.*, 2013]. These include the 30 Mile Bank fault, parts of the Santa Monica Bay detachment, and parts of the newly-mapped Catalina Island detachment (Fig. 1). These faults form a right-stepping linked system 200 km-long, that continues farther into Mexican waters. Above this fault system, a 100 km-long Oceanside "thrust" has been proposed, with the Carlsbad "thrust" above that [Rivero et al., 2000]. However, no evidence for contractional activity was interpreted on the central and southern parts of the Oceanside "thrust", and there is also little or no evidence for Quaternary deformation above its central part [*Campbell et al.*, 2009; *Sorlien et al.*, 2010; *Bennett*, 2012].

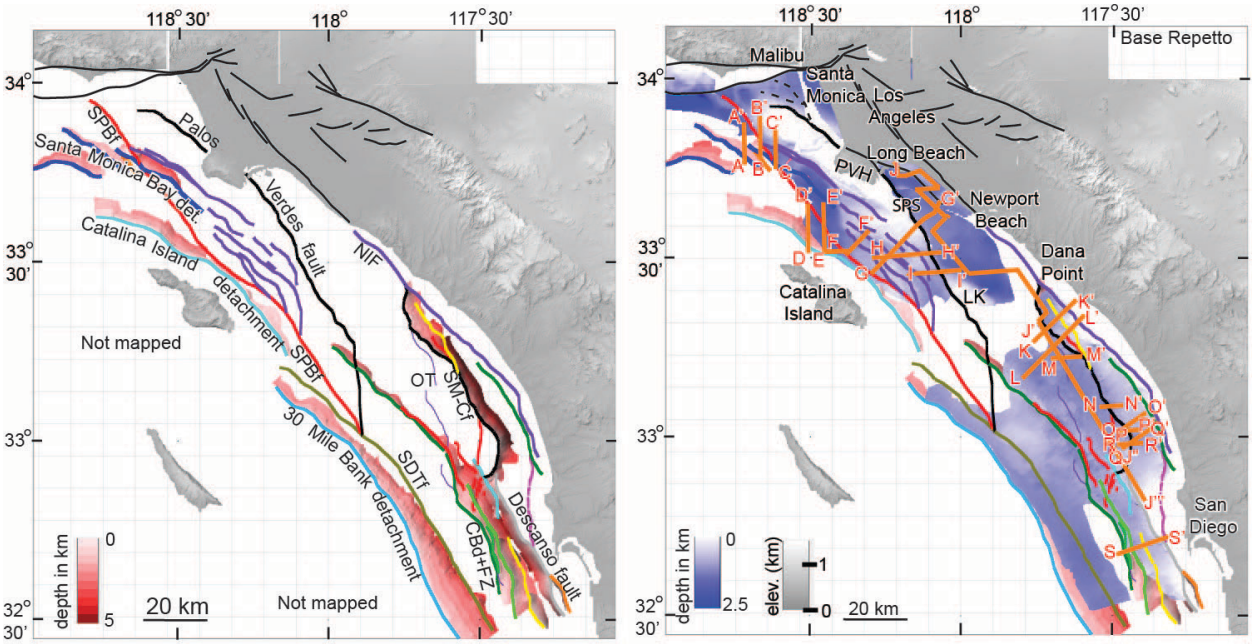

Figure 1: Left: A regional map of Quaternary faults indicating the names of the prominent offshore fault systems. Certain offshore faults are here newly mapped and others are from Sorlien et al. (2010). Onshore faults from *Wright* [1991] and *Plesch et al.* [2007]. Onshore faults are only included near Los Angeles, Long Beach, and Malibu. The thin purple lines indicate mapped locations of the Oceanside "thrust" (OT) of *Rivero et al.,* [2000] as represented by the Southern California Earthquake Center Community Fault Model [*Plesch et al.*, 2007], as modified by *Sorlien et al.* [2010]. CBd+FZ=Coronado Bank detachment+fault zone; NIF=Newport-Inglewood fault; SDTf=San Diego Trough fault; SM-Cf=San Mateo-Carlsbad fault; SPBf=San Pedro Basin fault. **Right:** Same faults obscured by blue shaded digital base Repetto (~4.5 Ma) or top Miocene horizons; the southern part of this surface could be younger than 4.5 Ma. Seismic reflection profiles A-A′ through S-S′ that are presented in later figures are located.

Several active right-lateral faults cut through this area. From west to east these include the San Diego Trough-San Pedro Basin fault [*Legg*, 1991; *Ryan et al.*, 2012; *Sorlien et al.*, 2006, 2013], the Palos Verdes fault [*McNeillan et al.*, 1996; *Brankman and Shaw*, 2009], and the Newport-Inglewood-Rose Canyon fault [*Yeats*, 1973]. Parts of the San Mateo-Carlsbad and linked

Descanso and Coronado Bank faults have been proposed to be right-lateral [*Nicholson et al.*, 1993], *Sorlien et al.*, 2010; *Bennett*, 2012].

Fault slip rate estimates derived from deformed sedimentary rocks require knowing the correct ages of the rocks. Recent publications and reports differ by up to a full order of magnitude on the ages of Quaternary reflectors [old: *Rivero and Shaw*, 2011; *Sorlien et al.*, 2010; *Bennett*, 2012: young: *Covault and Romans*, 2009; *Normark et al.*, 2009]. The studies that produced old age estimates used direct correlations to petroleum test wells, while the studies that produced young age estimates used extrapolation below shallow cores dated by the radiocarbon method. This extrapolation was guided by comparing seismic stratigraphy to the global sea level/climate record.

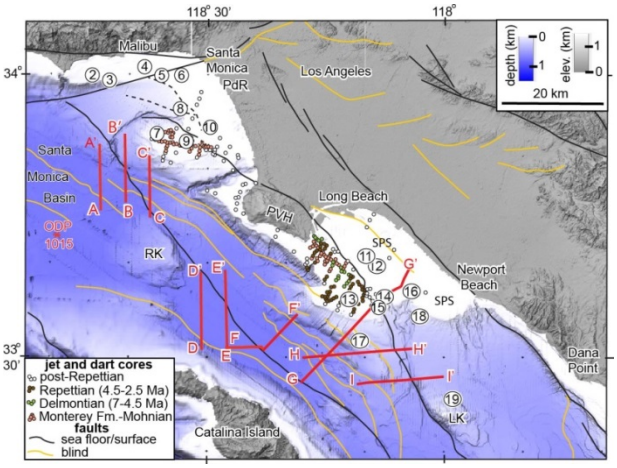

Figure 2: Multibeam bathymetry,topography, faults, and wells. Jet and dart cores from *Nardin and Henyey* [1978]. Bathymetric data from *Dartnell and Gardner* [1999]. Onshore faults from the Southern California Community Fault Model [*Plesch et al.*, 2007], except the Newport-Inglewood fault and a blind fault near Long Beach from *Wright* [1991]. Seismic reflection profiles shown in figures are located by labeled heavy red lines. Wells incorporated into this study and *Sorlien et al.* [2013] shown by numbered circles. Information on each well is given in the Supplemental Appendix 1 from *Sorlien et al.* [2013]. PdR=Playa del Rey; RK=Redondo Knoll, PVH=Palos Verdes Hills, SPS=San Pedro Shelf, LK=Lasuen Knoll. Figure modified from *Sorlien et al.* [2013].

We used multiple grids of recently released industry seismic reflection data [*Hart and Childs*, 2005], high-resolution U. S. Geological Survey seismic reflection data [*Sliter et al.*, 2005, 2010](Fig. 3), our compilation of bathymetry data (Fig. 2), logs and reports from petroleum test wells (Figs. 2, 3), and published sources to address these controversies. We produced digital depth-converted surfaces of many faults and several post-Miocene stratigraphic horizons. Simple modeling produced estimates of displacement on one of the faults.

2: Data and Methods of Analysis

2.1: Data Sources

Industry seismic reflection data acquired by Western Geophysical, Chevron, and Jebco, during the late 1970s through the 1980s were made publicly available in recent years through the National Archive of Marine Seismic Surveys (http://walrus.wr.usgs.gov/NAMSS/index.html). Acquisition of these profiles was designed to image deeply (5-6 km) and over a broad area (~30 km offshore) in order to fully characterize the petroliferous Miocene section and the Catalina schist basement. Higher resolution multichannel seismic profiles shot by the USGS in 1998, 1999, 2000, 2001, and 2006 were also utilized [*Sliter et al.*, 2005, 2010]. Point and multibeam

bathymetric data from *Dartnell and Gardner* [1999], and the National Geophysical Data Center (http://www.ngdc.noaa.gov/mgg/bathymetry/) were regridded.

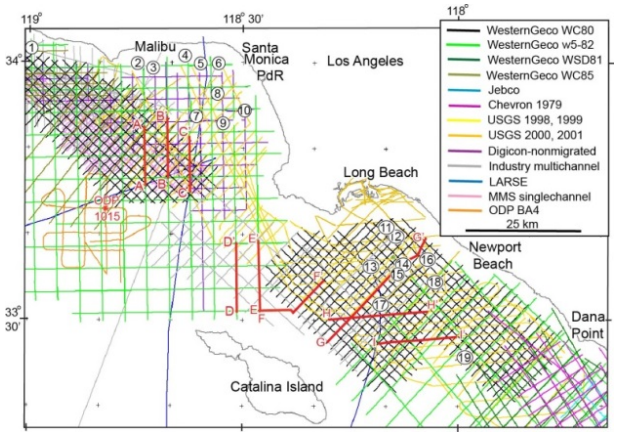

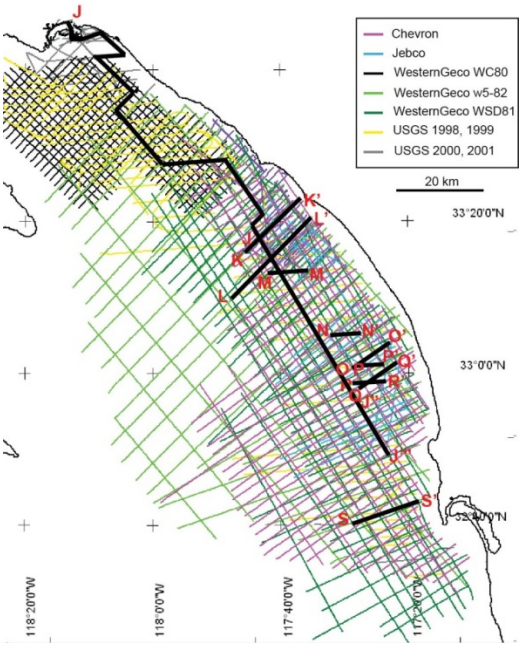

Figure 3: The data set of multichannel seismic reflection profiles, identified in the legend. Locations of figures given as labeled heavy Red (left) or black (right) lines. Left Figure modified from *Sorlien et al.* [2013]; right modified from *Bennett* [2012].

Age control needed to assess and constrain fault activity and related deformation was provided from data collected from deep-penetrating hydrocarbon wells including velocity surveys and Bureau of Energy Management (formerly Minerals Management Service) paleontology, and industry paleontology or picks from well reports, available for certain wells (supplementary appendix in *Sorlien et al.*, 2013). Deep scientific coreholes in and near Los Angeles and Long Beach Harbors provided detailed stratigraphy, especially since the last magnetic reversal about 780 ka [*Ponti et al.*, 2007; *Edwards et al.*, 2009; *Ehman et al.*, 2013].

2.2: Dataset Analysis - IHS Kingdom Suite

Our interpretation was carried out using interactive industry software designed for seismic reflection and well interpretation, "IHS Kingdom Suite". The aforementioned seismic reflection, bathymetric, and well data were uploaded into a Kingdom Suite interpretation project (*Alward et al.*, 2009; *Campbell et al.*, 2009; *Sorlien et al.*, 2010, this project). In order to test the accuracy of the navigation for the seismic reflection data, bathymetric grids were converted to two-way travel time using an interval velocity of 1,490 m/s, and displayed on the MCS profiles. The Chevron data did not have useable shot or CDP numbers in the trace headers, and the navigation shot-trace number correspondence for the Western w5-82 data was complicated and often needed additional shifting. The navigation shot/data trace correspondence was then adjusted until a good visual match was obtained between the seafloor reflection and the time-converted bathymetry.

2.3: Structural and Stratigraphic Interpretation

Loop-tying techniques through MCS profiles spaced at 1 to 2 km serves as a type of error analysis. Loop-tying involves the geometrical fact that rock interfaces and faults should be at the same depth at the intersections of two planes. The reality for 2D MCS data is a bit more complicated. Vertical and horizontal shifts stemming from 2D migration of dipping strata as well as the disparate resolutions of the various data sets were accounted for in the interpretations. Although submarine fans involve localized sedimentation [*Covault and Romans,* 2009], reflections could be correlated between fans. This may be partly due to regional hemipelagic deposition in addition to turbidites, and to structural and sea level/climate control on some of the interpreted sequence boundaries/unconformities.

Non-vertical faults can also be "tied" through intersecting strike and dip lines. Because of 2D migration effects, moderately-dipping faults can have large mis-ties between strike and dip lines, especially at deeper travel times. Fault positions were carefully interpreted on the dip lines. The faults were drawn on the strike lines through there intersections on the dips lines. Where there are strong reflections from the fault surfaces, these reflections are shallower on the strike lines than on the dip lines. Thus, on strike lines faults are interpreted through their ties from the dip lines, below their reflections. Sub-vertical faults such as parts of the San Pedro Basin fault or parts of the Newport-Inglewood fault can be interpreted by comparison without "ties".

There are many dozens, perhaps hundreds of minor faults imaged on the MCS data, active before the 1.95 Ma top Lower Pico or before the older H4, that we did not map. Long, regional faults such as the San Mateo-Carlsbad or the Palos Verdes fault can have up to a dozen strands within a zone. Within a fault zone, we generally mapped the lowest fault that deformed Quaternary strata, and did not interpret smaller, but potentially active strands, even if they deformed the sea floor. Examples include the main Carlsbad fault on P-P' vs. minor young faults above it, The Palos Verdes fault on G-G', and the Newport-Inglewood fault on L-L' (locations on Figures 1, 3). Many of the shallow faults project downward to intersect and merge with the faults we mapped and represented as 3D depth-converted grids.

2.4: Gridding

Once the fault interpretations were smoothed and modified for quality and consistency, either 500 or 200 m two-way travel time grids were created to produce continuous surfaces with few artifacts. These were then regridded at 100 m for better display and smoother edges where trimmed at upper edges and the bottoms edges of interpretations. Stratigraphic horizons were generally gridded at 200 m and regridded at 100 m. The four late Quaternary "Q" Horizons were gridded in Kingdom Suite using "flex grid" whereas top Lower Pico and H4 as well as the fault surfaces were gridded using "Projection of Slopes" in Surface III (*Kansas Geological Survey*).

2.5: Depth Conversion

The time gridded fault surfaces and horizons were depth-converted by producing velocity maps based upon time-depth charts constructed in Kingdom Suite. The input data were

generated from CVM-H provided by the Southern California Earthquake Center [*Suss and Shaw*, 2003]. CVM-H is the Harvard version of the SCEC Community Velocity Model (CVM). CVM-H has been constructed from velocity analysis by industry during processing of MCS data. It also includes many direct velocity surveys from boreholes [*Suss and Shaw*, 2003]. However, there are few wells south of San Pedro shelf so we assume CVM-H there is based almost entirely on velocity analysis during processing of MCS data. CVM-H requires coordinates and seafloor depth in order to generate a velocity profile for that specific location. Eighty locations were processed in the velocity generating software to create time-depth charts [*Bennett*, 2012]. This provided the basis for depth-converting the interpreted stratigraphic and structural interpretations. (For more information on this model please refer to the Southern California Earthquake Center website: http://structure.harvard.edu/cvm-h).

One dimensional velocity models were used for depth conversion of San Pedro Shelf, northern San Pedro basin, and Santa Monica Bay, as explained in *Sorlien et al.*, [2013].

2.6: Cross-Sections

Cross-sections were extracted through the gridded fault and stratigraphic depth surfaces at an azimuth of 64°, which is perpendicular to the approximate strike of the San Mateo-Carlsbad fault north of its northern big bend. In all, fifty-eight sections were drawn with each spaced 1 km apart. Additional cross sections were drawn in 5 km increments to illustrate fault geometries of the faults adjacent to San Diego.

2.7: Trigonometric displacement modeling.

Displacement modeling for the San Mateo-Carlsbad involved measuring the structural relief of top lower Pico and the strike and dip of the fault at each of the 58 cross sections. We assume that the hanging-wall moved simply (obliquely) up or down the footwall (Fig. 4)[*Sorlien et al.*, 2006]. For certain fold models, the structural relief due to folding can be more than, even double, the vertical motion. If such folding occurred, we would overestimate the displacement. A range of displacement directions of the hanging-wall with respect to the footwall are modeled, with each direction also including a range of magnitudes. Then, the modeled deformation along the fault, through bends, is compared to the measured values.

The San Mateo-Carlsbad fault consistently dips to the east; therefore, the footwall is always to the west and hanging wall to the east. The measurements of structural relief of top Lower Pico involved:

1) Carry out a visual inspection of the depth-converted profile to determine if vertical separation is normal or reverse.

2) If reverse separation is observed, the highest point of the hanging wall within 4 km from upper fault tip is measured and the depth of the lowest point on the footwall within 2 km of the fault tip is recorded. The vertical relief is the difference between the two depths.

If normal separation is observed, the measurements are reversed: measure depth of lowest point of the hanging wall within 2km of the fault tip. These distances were chosen because they

visually best captured structural relief related to the shallow part of the San Mateo-Carlsbad fault.

Apparent dip for the San Mateo-Carlsbad fault was calculated by measuring the depth of the tip of the fault and the depth of the fault 4,000 meters east of the tip on each of the 58 cross sections. Strike of the San Mateo-Carlsbad fault was measured on the 2500 m depth contour at each designated cross section. Strike was then interpolated linearly at 200m increments.

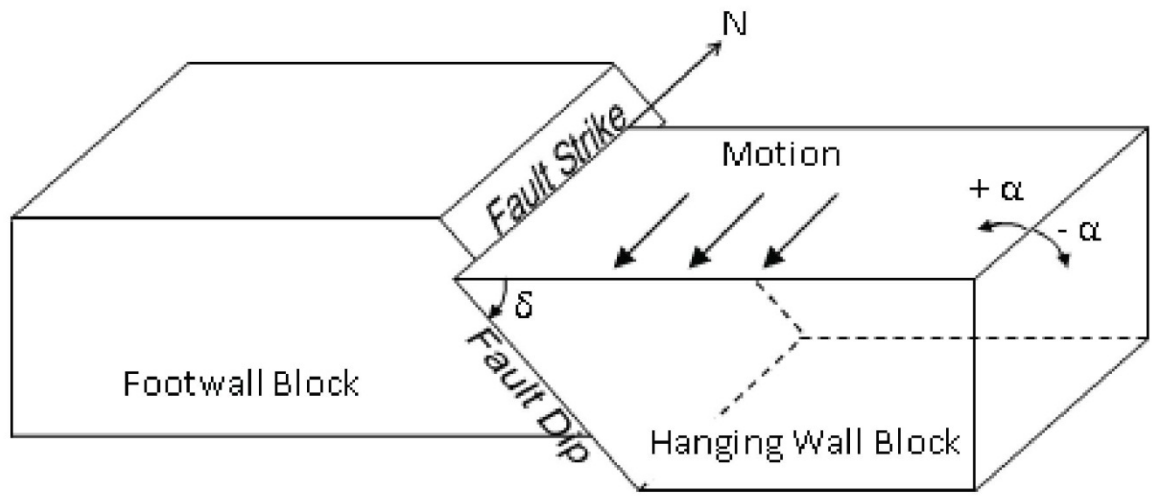

Figure 4: A graphical representation for the values in the slip modeling equation $SR=\Sigma_i 1km*\sin(\alpha_i)*\tan(\delta_i)$. This idealized graphic assumes that relative plate motion accommodated by the fault is expressed by movement of the hanging wall block in a predominantly southward motion. From *Bennett* [2012].

Measurements of fault strike and apparent fault dip are compiled into an Excel spreadsheet to calculate the true fault dip of the SMC fault for each cross-section. In turn, these values are used to trigonometrically calculate the expected magnitude of vertical deformation for varying values of the horizontal slip direction and magnitude of the hanging wall with respect to the footwall:

$$SR=\Sigma_i 1km*\sin(\alpha_i)*\tan(\delta_i)$$

Where α_i is the angle between the local slip vector and local fault strike, and δ_i is the fault's true dip for cross-section (Fig. 4). The slip direction of the hanging-wall, fault strike, and fault dip are used for each interpolated 200 m bin along the fault to calculate increase in structural relief for rock passing through each bin.

2.8: Comparison post-1950 ka vs. post-~600 ka deformation.

For the late Quaternary Q3 and Q4 horizons (Fig. 5), vertical deformation across the fault is less than 350 meters and does not extend that far from the San Mateo-Carlsbad fault. Because of this small relief and the possibility of deposition at significantly different depths across the fault trace (expected for the Q1-Q4 strata), and because it was only possible to completely interpret

horizons over about 25 km of the hanging-wall of San Mateo-Carlsbad, trigonometric modeling to infer cumulative slip is not expected to be very reliable for these two horizons. The horizontal distances used for depth measurements were 2 km for the hanging-wall and 1 km for the footwall, and top Lower Pico was also re-measured at these distances.

Thus, the main goal in measuring structural relief of the Q horizons is to test whether the overall deformation pattern is similar to that of the deeper top Lower Pico horizon - or not. If the deformation pattern is similar, it would support a model where the tectonic regime has not changed significantly since deposition of top Lower Pico, and that long term slip directions and rates might therefore extend into the present. In other words, this fault would be an active fault, and the mean slip rate inferred from modeling the deformation of top Lower Pico are likely applicable to the Present.

2.9: Sources of Error

Error in the two-way-travel-time structural and stratigraphic interpretations was minimized during this study by being consistent, systematic, and thorough during each step used in the methods. The CVM-H velocity model is based upon stacking velocities for the study area (Suss & Shaw, 2003) and so may contain significant error. The trigonometry used in the slip modeling assumes that the hanging wall is moving rigidly up the apparent dip of the footwall. If the actual structural model for the San Mateo-Carlsbad fault is a fault-propagation fold where the forelimb is wider at top Lower Pico than at depth closer to the fault, then our model over-estimates displacement. Unconformities can be time transgressive and therefore may be of slightly different age in the basin than where dated at wells or cores. Even so, each method of analysis is easily reproducible; therefore, we remain confident that the results produced by this study are based on thorough analyses that have taken into account the aspects of the methods susceptible to error.

2.10: Stratigraphic Interpretation

In order to resolve the up to an order of magnitude disagreement between old [*Rivero and Shaw*, 2011; *Sorlien et al.*, 2010] and young (*Covault and Romans*, 2009; *Normark et al.*, 2009] age interpretation for stratigraphic horizons, we used high-resolution seismic reflection data from 2000 and 2001 to correlate directly to scientific coreholes in Long Beach harbor that were extensively analyzed in several papers (Figs. 5, 7)[*Ponti et al.*, 2007; *Edwards et al.*, 2009; *McDougall et al.*, 2011; *Ehman et al.*, 2013]. In addition, we revisited our earlier correlations to industry wells with Bureau of Energy Management paleontology, and published and unpublished additional age control, on San Pedro Shelf (Fig. 6)[appendix in *Sorlien et al.*, 2013]. This included use of dated coastal stratigraphic sections reported in *Blake* [1991].

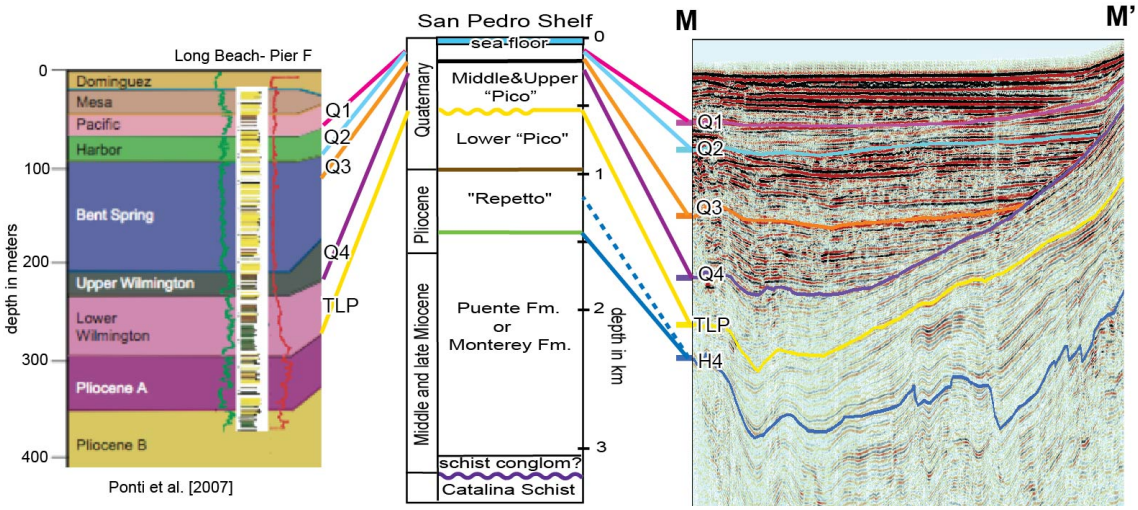

Figure 5: USGS high resolution multichannel seismic reflection profile 217 showing the interpreted Quaternary horizons relative to one another located in the footwall southwest of the San Mateo-Carlsbad fault. The blue Q2 and the orange Q3 in this figure are not the same horizons as the blue "Pico" unconformity and the orange "Hueneme" in Figure 6. Quaternary 4 here is a major onlap surface representing increasing missing section to the right (east). The stratigraphic column in the center is modified from Wright (1991) for the downthrown northeast side of the Palos Verdes fault on San Pedro Shelf, south of Long Beach. The Quaternary horizons were correlated as part of this project to a scientific core hole on Pier F of the port of Long Beach, that was presented by *Ponti et al.* [2007] and *Edwards et al.*, [2009] (Far Left). Refer to Figures 1 and 3 for location of M-M'. Figure modified from *Bennett* [2012].

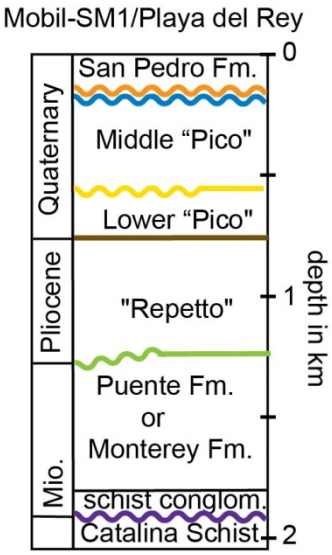

Figure 6: Stratigraphic column, located on Figure 2; Mobil SM1 is Well 6. Depths from well Mobil SM-1 and the Playa del Rey field. From *Sorlien et al.*, [2013] originally drawn from *California Division Oil, Gas, and Geothermal Resources* [1992]. Orange is the "Hueneme" unconformity and blue is the "Pico" unconformity. These unconformities need not correspond to the "Q" unconformities in Figures 5, 7, etc.. In the area of well Mobil SM1, strata above the Hueneme unconformity may postdate 125 ka, and those just below the Pico unconformity may be as old as 1 Ma.

The published young age model of *Covault and Romans* [2009] is compared to our results using the same part of the same MCS profile at the same scale in Figure 8. Our 1950 ka top Lower Pico horizon is over an order of magnitude older than interpreted by *Covault and Romans* [2009], and our Q1 through Q4 sequence boundaries are several times older. The age of folded, offset, and tilted strata is directly related to fault slip rates, and so if the young age model was correct, this would have dramatic implications for earthquake hazard.

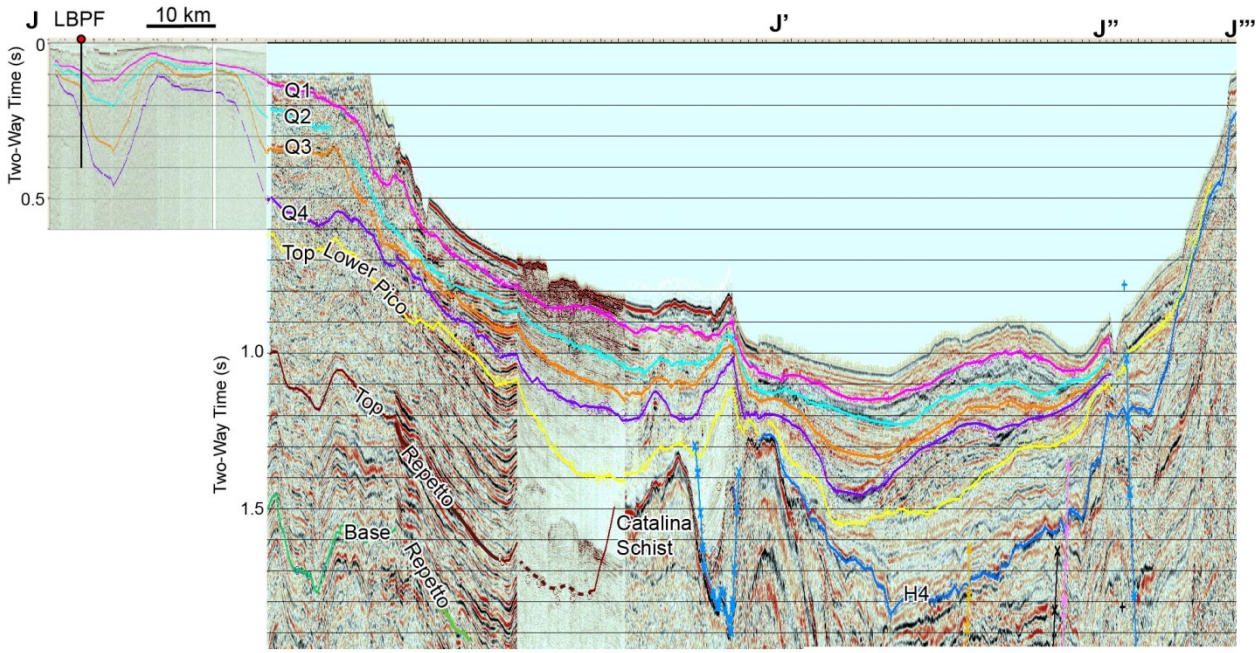

Figure 7: A composite profile through different multichannel seismic reflection (MCS) datasets, illustrating the 120 km N-S extent of the stratigraphic interpretation of top Lower Pico (yellow) up through Q1 (magenta). Stratigraphic horizons are labeled. A scientific corehole from Pier F in Los Angeles harbor is shown at the north end of the profile (LBPF). Age and velocity information from *Ponti et al.* (2007) and *Edwards et al.,* (2009) were used to correlate the LBPF stratigraphy to the seismic reflection data. Top Lower Pico and top and base Repetto horizon from oil exploration wells and published cross sections were correlated to the northern half of this profile (appendix in *Sorlien et al.,* 2013). The small color circles along each horizon interests represent the numerous intersections ("Ties") to crossing MCS profiles. A single profile through dense grids of MCS data can never adequately represent the actual error-checking of careful work through a volume of data. Refer to Figures 1 and 3 for profile location. Figure modified from *Bennett* [2012].

The Blue (H4), horizon interpreted throughout the southern part of our study area could not quite be directly correlated to wells on San Pedro Shelf, but appears to be close in stratigraphic position to the 4500 ka base Repetto (Figs. 5, 8). Comparison of the interpretation of MCS profiles in *Rivero and Shaw* [2011] to nearby MCS profiles with our interpretations suggests that our H4 is near and below their top Repetto, including near their top Capistrano Formation. We cannot rule out our H4 being significantly younger than 4,500 ka.

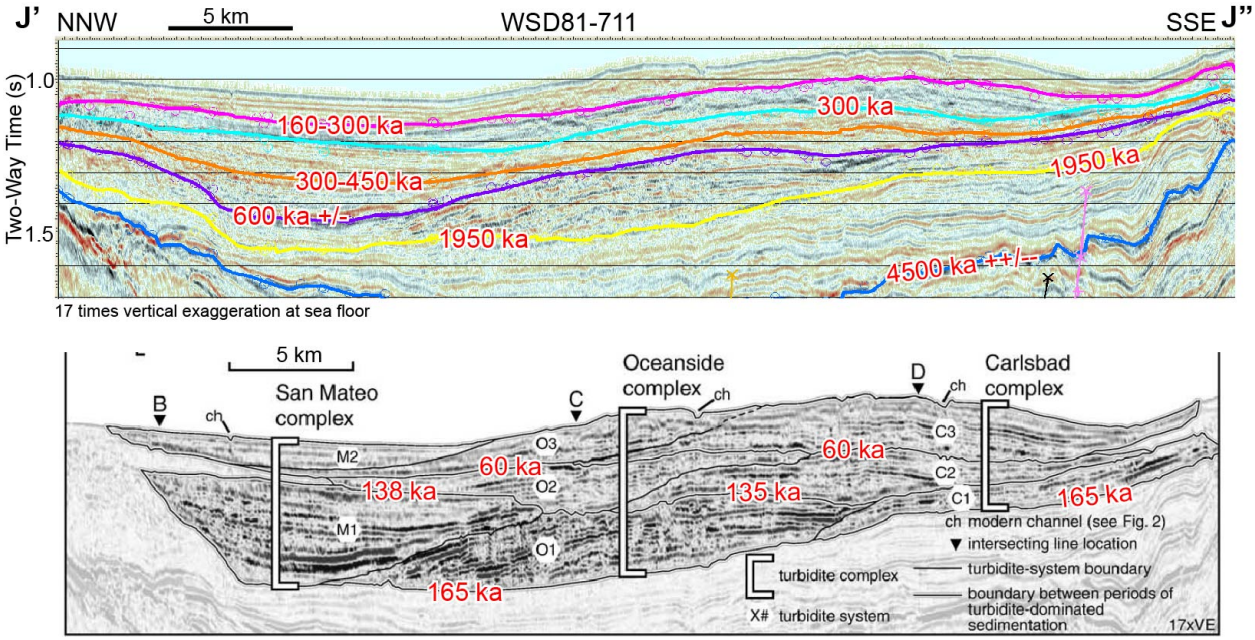

Figure 8: Above: The J'-J'' part of the profile shown in the previous Figure (Fig. 7). It has the same colors for stratigraphy, and less vertical exaggeration. Located on Figures 1 and 3. The top version is our interpretation and the bottom version is from *Covault and Romans* [2009], with addition of ages using the *Covault and Romans* [2009] interpretation and the Oxygen isotopic age model from *Lisiecki and Raymo* [2005]. The horizontal scale was corrected from 4 km to 5 km. Our stratigraphic age model for this area (top) ranges from several times older to over an order of magnitude older than the age model displayed on the lower figure. Figure modified from *Bennett* [2012].

3: Results

3.1: Descriptions

Our results include detailed fault and fold geometry as well as several late Quaternary stratigraphic horizons for the area between Long Beach and San Diego, within 20 to 30 km of the coast. This continued the work of *Sorlien et al.* [2010] with Pliocene to early Quaternary horizons within 30 to 45 km of the coast. This work was funded by this USGS grant, and includes displacement modeling on the San Mateo-Carlsbad fault. This work documents a boundary near 33° N latitude between Quaternary transpression (north) and transtension (south). During the period of this grant, months of time were spent revising a now-published paper, originally funded by the Southern California Earthquake Center, which covers the area to the northwest. These revisions included new interpretations and figures and detailed work on stratigraphy [*Sorlien et al.*, 2013]. Combining some of this work into this report provides context to the extent of Quaternary thrust activity on a giant system of Miocene low-angle (oblique) normal faults that are present for over 200 km from Santa Monica Bay to the offshore USA-Mexican border (Figs. 1, 9). We see no evidence for significant Quaternary shortening south a line starting from a bend in the San Mateo-Carlsbad fault at 33° N latitude and continuing to the west-southwest. This bend is the northern end of an 18 km right-releasing stepover between the San Mateo-Carlsbad-Newport-Inglewood positive (transpressional) flower structure to the north and the Coronado Bank-Descanso negative (transtensional) flower structure to the south.

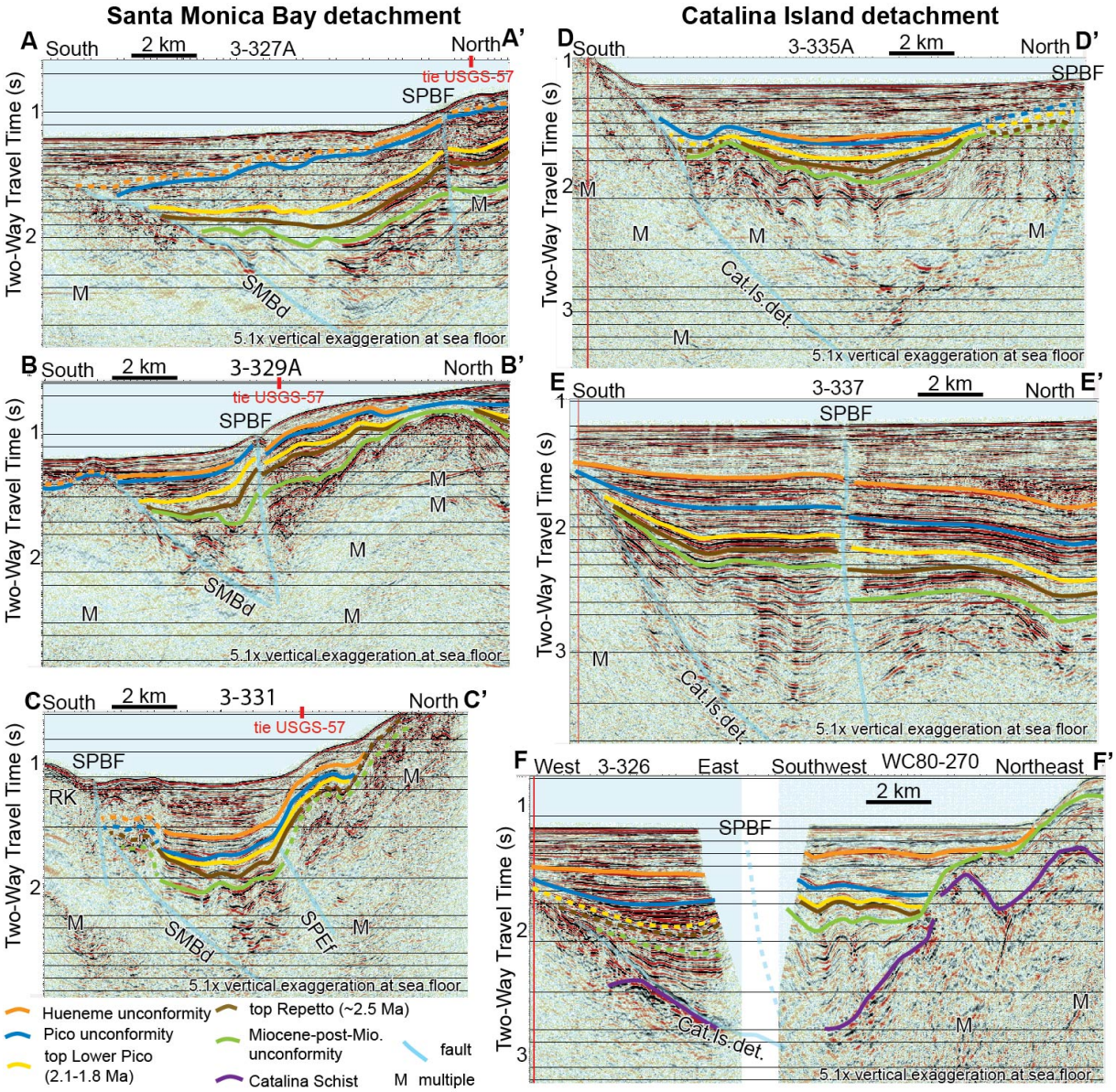

Figure 9: Migrated multichannel seismic reflection profiles provided by Western Geophysical, from the U.S. Geological Survey NAMSS website [*Hart and Childs*, 2005], located in Figures 1, 2, and 3. The column on the left presents profiles across the Santa Monica Bay detachment. A-A′ images minimal thrust reactivation in the west (upper left), while on C-C′, the Palos Verdes anticlinorium is folding above it (lower left). The column on the right presents profiles across Catalina Island detachment. E-E′ images minimal thrust reactivation in the west (center right); while Palos Verdes anticlinorium is folding above this fault on F-F′ in the east (lower right). The right-lateral San Pedro Basin fault is imaged on every profile. The intersection ("tie") of profiles on the left with USGS-57 are labeled; USGS-57 is a figure in *Normark et al.* [2006]. The range of likely ages for the Hueneme and Pico unconformities is discussed in Section 2 of *Sorlien et al.*, [2013]. Cat. Is. Det.=Catalina Island Detachment; M=Multiple reflection; RK=Redondo Knoll; SPBF=San Pedro Basin fault; SPEf=San Pedro Escarpment fault. Figure from *Sorlien et al.* [2013].

Industry MCS data in Figure 9 image the gently-dipping Santa Monica Bay and Catalina Island detachments. The upper edges of the Miocene faults have not been significantly re-activated, except for on D-D′, where thrust-folding may be related to a local bend in the right-lateral San Pedro Basin fault (SPBF). Downdip and to the southeast, these faults are over-ridden by Palos Verdes anticlinorium and thus have been (oblique) thrust reactivated. G-G′ on Figure 10 images the southern part of Palos Verdes anticlinorium, cut by the Palos Verdes fault, as well is some Miocene normal faults reactivated in transpression. Stratigraphy constrained by wells on San Pedro Shelf was correlated across the Palos Verdes fault by comparison of the reflection pattern on H-H′ and other high-resolution USGS profiles (Fig. 11). Initiation of folding beneath San Pedro escarpment is synchronous with deposition of the 1.95 Ma top Lower Pico in this area (Figs. 10, 11)[*Sorlien et al.*, 2013]. This is based on parallel reflections below top Lower Pico and fanning of dips and onlap above (Fig. 12).

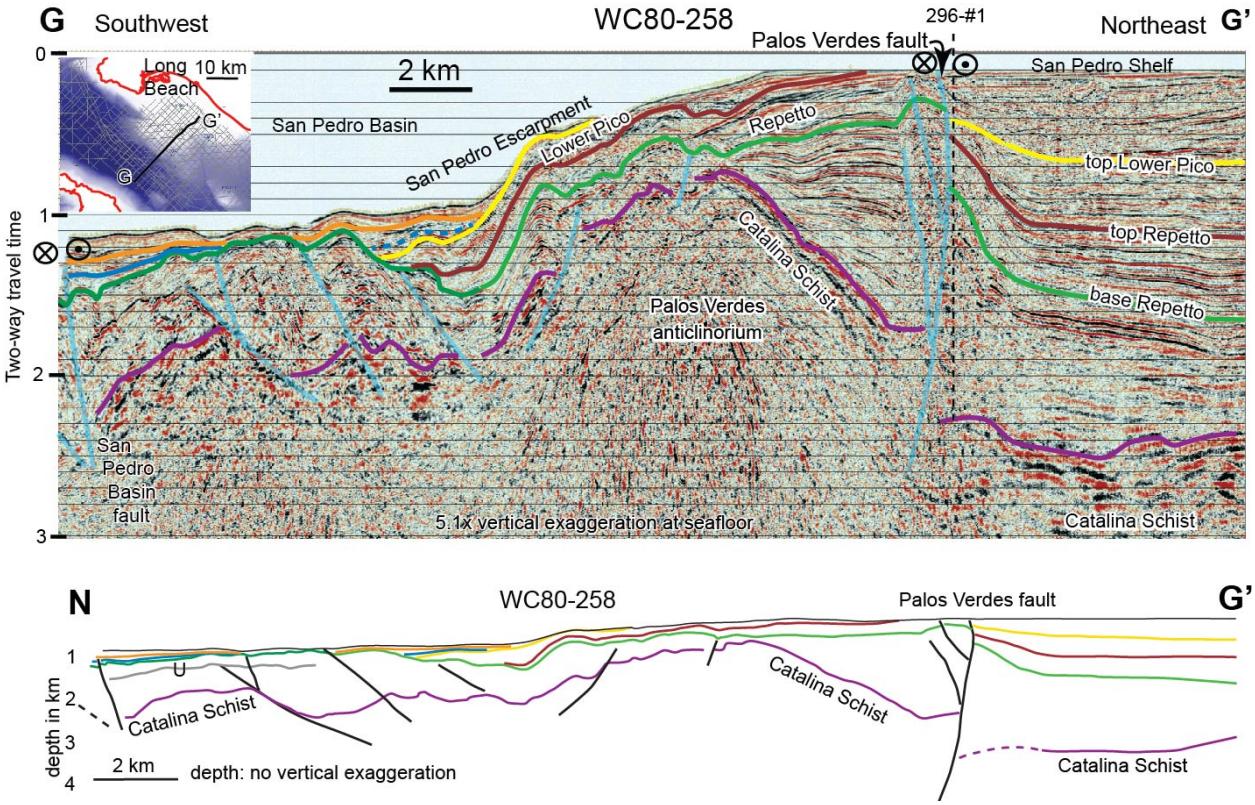

Figure 10: G-G′, presented in two-way travel time and in depth. Located on inset and Figures 1, 2, and 3. Thinning of Pliocene (and probably Miocene) strata to the southwest suggests reversals of dip-slip sense and basin inversion. Strong basement reflection on either side of Palos Verdes fault is Catalina Schist [*Wright*, 1991; *Sorlien et al.*, 2013], although Miocene volcanic rocks are also present in the area [*Dibblee*, 1999; *Fisher et al.*, 2004]. The blue and orange horizons are respectively the Pico and Hueneme unconformities as in Figures 6, 9 and 11. Figure from *Sorlien et al.* [2013].

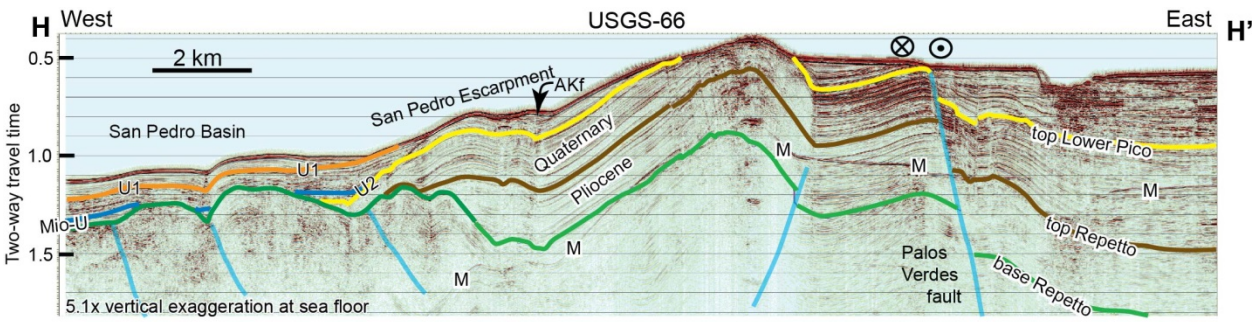

Figure 11. Migrated USGS multichannel seismic reflection profile H-H', located on Figures 1, 2, and 3. Data from *Sliter et al.,* [2005]. Pliocene and part of lower Quaternary strata do not thin across the southwest limb of the PVA, while younger Quaternary strata onlap it and date initiation of folding here. The entire Pliocene section pinches out beneath the modern bathymetric basin at the west end of profile, which is interpreted as the footwalls of NE-dipping Miocene normal-separation faults. The right-lateral Palos Verdes fault dips northeast away from the crest of the anticlinorium and has normal separation, and thus does not explain the folding. The southwest-dipping blind fault does not extend far along strike (Figure 1).The NNW-striking Avalon Knoll fault (AKf) of *Marlow et al.* [2000] here lacks vertical separation of Pliocene strata, and is likely a minor structure and/or a newly-developed fault. Figure from *Sorlien et al.* [2013].

Profile I-I' (Fig. 12) is included to show evidence for tilting, and the existence of a planar angular unconformity (U3) just above top Lower Pico, now at 650 m water depth. If this unconformity was wave eroded, subsidence rates would have been in excess of 0.28 mm/yr. in this area [*Sorlien et al.*, 2013; see also *Fisher et al.,* 2004]. Documentation of footwall subsidence is important to the evaluation of blind thrust hazard, because subsidence must be combined with hanging wall vertical motion to produce estimates of growth of structural relief. It is growth of structural relief, not rates of surface uplift, that must be used in models for thrust slip rates [e.g., *Pinter et al.*, 2003].

The remaining figures of seismic reflection profiles were interpreted and created as part of this USGS-funded project. K-K' and L-L' in Figures 13 and 14 image the northern part of The San Mateo-Carlsbad-Newport-Inglewood fault. These faults project to intersect at depth, and thus are a "flower structure" characteristic of strike-slip fault systems [e.g., *Sylvester*, 1988]. Quaternary folding is contractional, and thus this is a positive flower structure. Shallow likely Catalina Schist and thin to missing Miocene strata is imaged on MCS data in the footwall of the San Mateo-Carlsbad fault. This compares to at least 2 km thickness of Miocene rocks in a well close to the northeast end of L-L' [*Crouch and Suppe*, 1993], and is consistent with fault reactivation and basin inversion. The Oceanside thrust of *Rivero et al.* [2000] coincides with our San Mateo-Carlsbad fault on K-K' and is beneath it on L-L', but their mapped fault trace diverges southward from our San Mateo-Carlsbad fault (Fig. 1)[*Rivero et al.,* 2000; *Rivero and Shaw*, 2011].

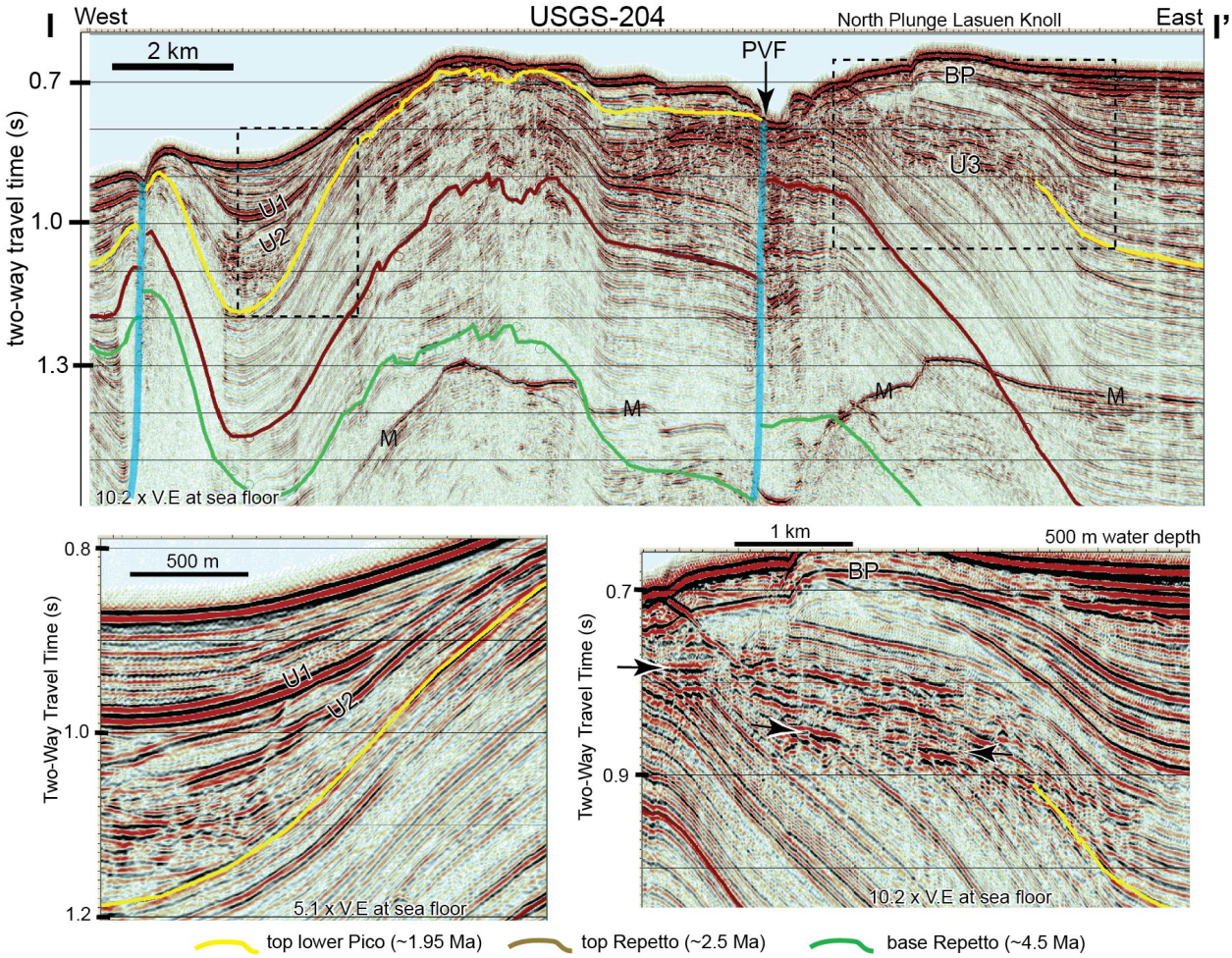

Figure 12: Migrated seismic reflection profile I-I' across the south plunge of the Palos Verdes anticlinorium and Palos Verdes fault (PVF), south of San Pedro Shelf, located on Figures 1, 2, 3. The strata below the ~1.95 Ma yellow horizon are fully-involved in the folding and thus the western fold limb did not start folding until that time. Lower Left: part of profile displayed at half the vertical exaggeration and located by dashed black rectangle. Progressive tilting of late Quaternary turbidites and of sequence boundaries U2 and U1 is consistent with ongoing growth of the anticlinorium. The Hueneme and Pico unconformities cannot be correlated this far south with data available to us, but by comparison to Figure 9, U1 could be the Hueneme unconformity. Lower Right: part of profile located by dashed black rectangle. Black arrows indicate angular unconformities; the lower one, now at 650 m depth, represents about 550 m of subsidence if wavecut during low sea level. The Palos Verdes fault exhibits down-to-the-west stratigraphic separation, opposite of the separation farther north. "BP"=Bubble Pulse reflection ("ghost") related to airgun source. Data from *Sliter et al.* [2005]; Figure from *Sorlien et al.* [2013].

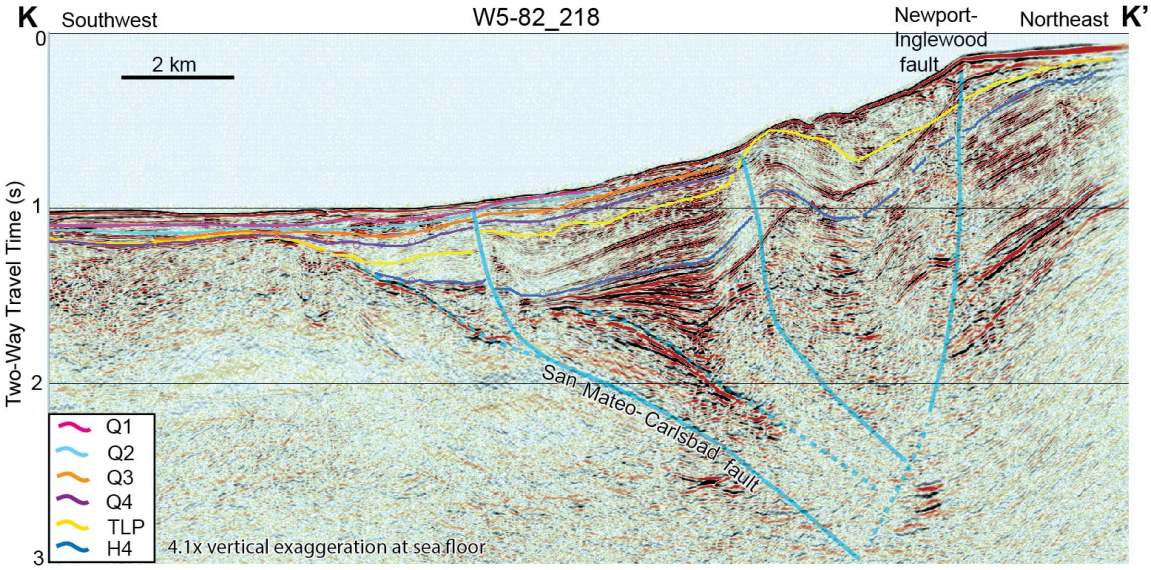

Figure 13: Western Geophysical Company 3-218 displayed as profile K-K'; located on Figures 1, 3. The San Mateo-Carlsbad fault forms a positive flower structure with the Newport-Inglewood and intervening faults north of a major right-step over to the negative flower structure. TLP=top Lower Pico.

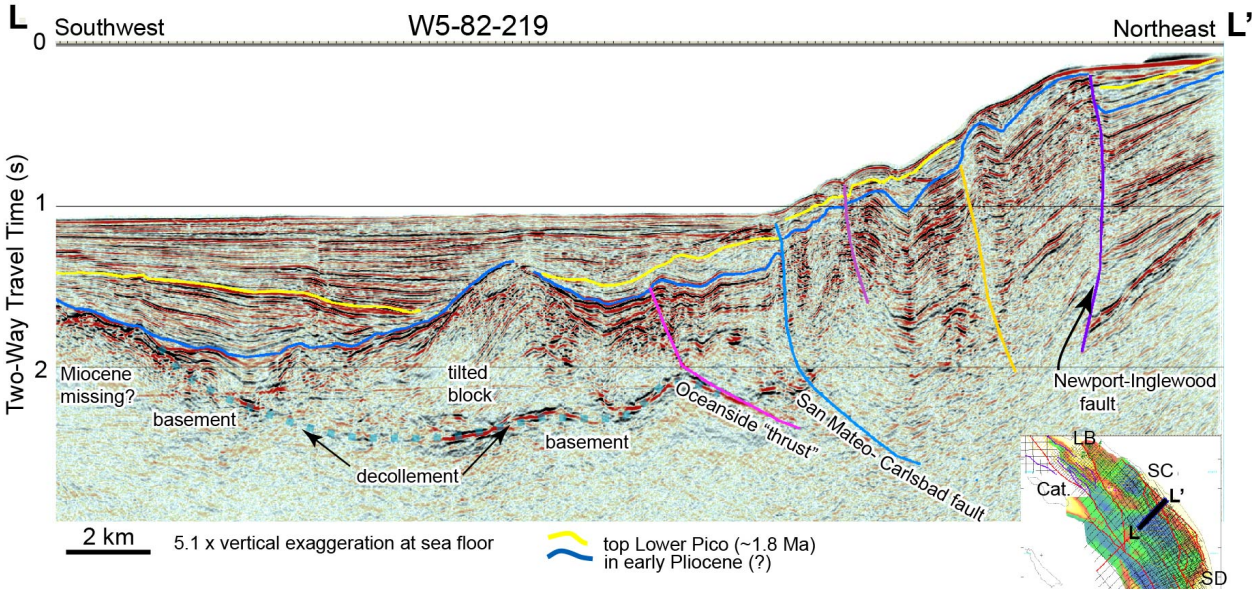

Figure 14. A Miocene low-angle normal fault system dips northeast beneath the shelf and slope. It is reactivated, with slip being incompletely partitioned between the right-lateral Newport-Inglewood fault and the oblique right-reverse San Mateo-Carlsbad fault [*Campbell et al*., 2009]. Dashed cyan is a Miocene extensional decollement responsible for tilting of the labeled block. The along-strike Mobil Oceanside well indicates that the imaged sedimentary section near the Newport-Inglewood fault down to at least 1.5 s two-way travel time is Miocene. The shallow basement beneath the bathymetric basin leaves little room for Miocene strata. Located on Figures 1 and 3, and on the inset. The inset shows sub-bottom structure from *Sorlien et al.* [2010]. Cat.=Catalina Island, LB=Long Beach, SC=San Clemente, SD=San Diego.

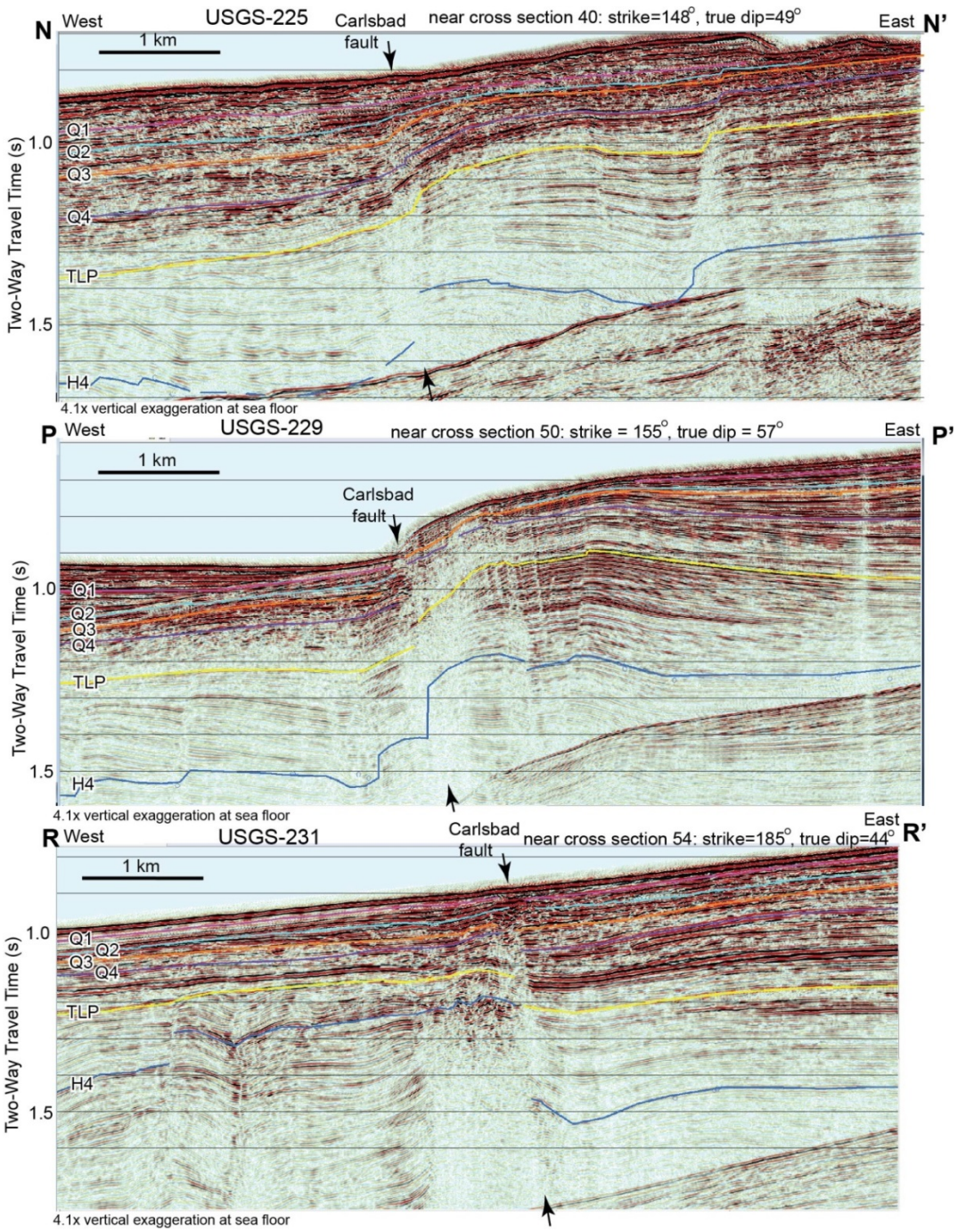

Figure 15: USGS high resolution multichannel seismic reflection profiles showing interpreted stratigraphy across the San Mateo-Carlsbad fault (arrows). Located on Figures 1, 3. The local strike azimuths and true dips are labeled above each profile: southeast strikes of 148 and 155 are restraining and the N-S strike of 185 is releasing for right-lateral motion, as seen by the reverse component on N-N′ and P-P′ and the normal-separation on R-R′. Less structural relief is exhibited by the shallower horizons, indicating steady sedimentation during San Mateo-Carlsbad fault activity. The Top Lower Pico (TLP) unconformity caps normal-separation faults in the footwall southwest of the San Mateo-Carlsbad fault, indicating an end to regional transtension in this area at ~1.95 Ma [*Campbell et al.,* 2009].

N-N′ through R-R′ image a change from reverse-separation and contractional folding to normal separation through a bend in the San Mateo-Carlsbad fault from a northwest strike to a north strike (Figs. 15, 16). The high-resolution USGS MCS data [*Sliter et al.*, 2005] in Figure 15 also demonstrate that the Top Lower Pico (TLP) through Q1 horizons can directly be correlated across the fault on N-N′, and then correlated on both sides of the fault along numerous MCS profiles of different orientations. Cross sections through the depth-converted fault and stratigraphic surfaces in Figure 18 present this geometry in systematic fashion.

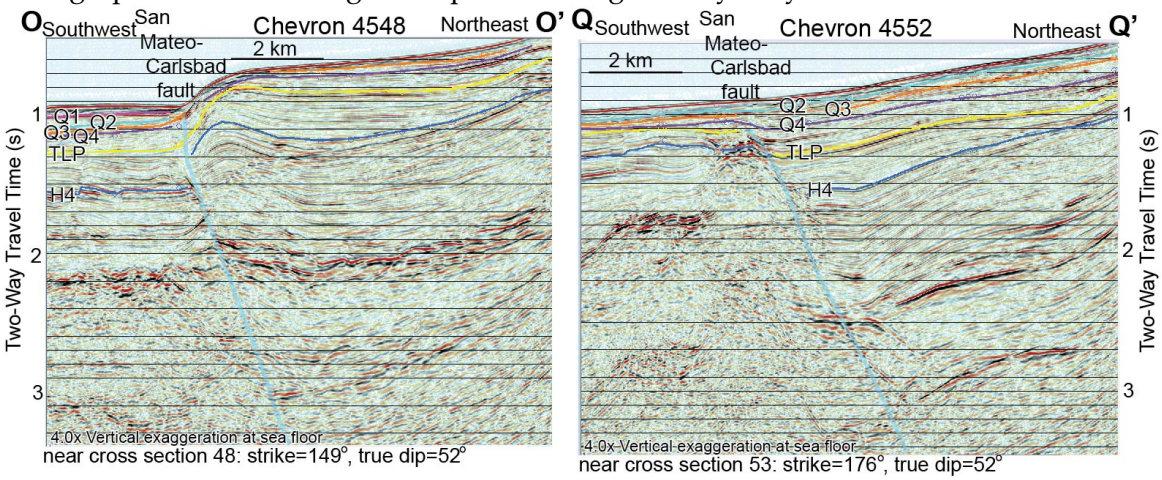

Figure 16: Migrated Chevron profiles located near the northern bend in the major right stepover between the San Mateo-Carlsbad fault and the Descanso and Coronado Bank faults. All interpreted horizons on Q-Q′ exhibit normal separation, just 5 km south of O-O′, where they exhibit reverse separation. This change is consistent with right-lateral faulting. Refer to Figures 1, 3 for location.

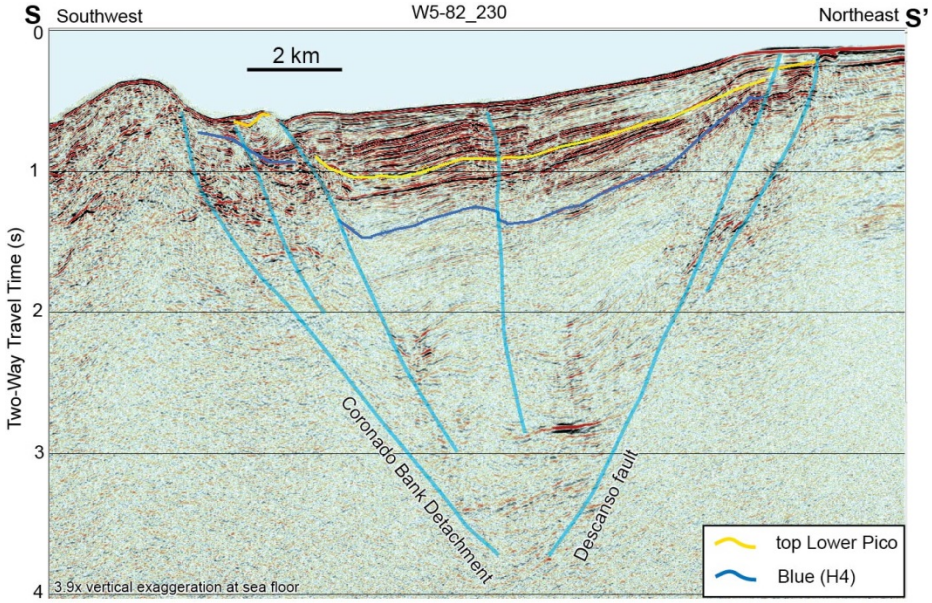

Figure 17: Western Geophysical Company profile displayed as S -S′. A negative (transtensional) flower structure geometry is imaged adjacent to San Diego. Located on Figures 1 and 3. The late Quaternary "Q" horizons could not be correlated this far southeast, and the top Lower Pico and H4 horizons cannot be interpreted and/or are eroded from the footwalls. Therefore we have not been able to model displacement for these assorted fault strands.

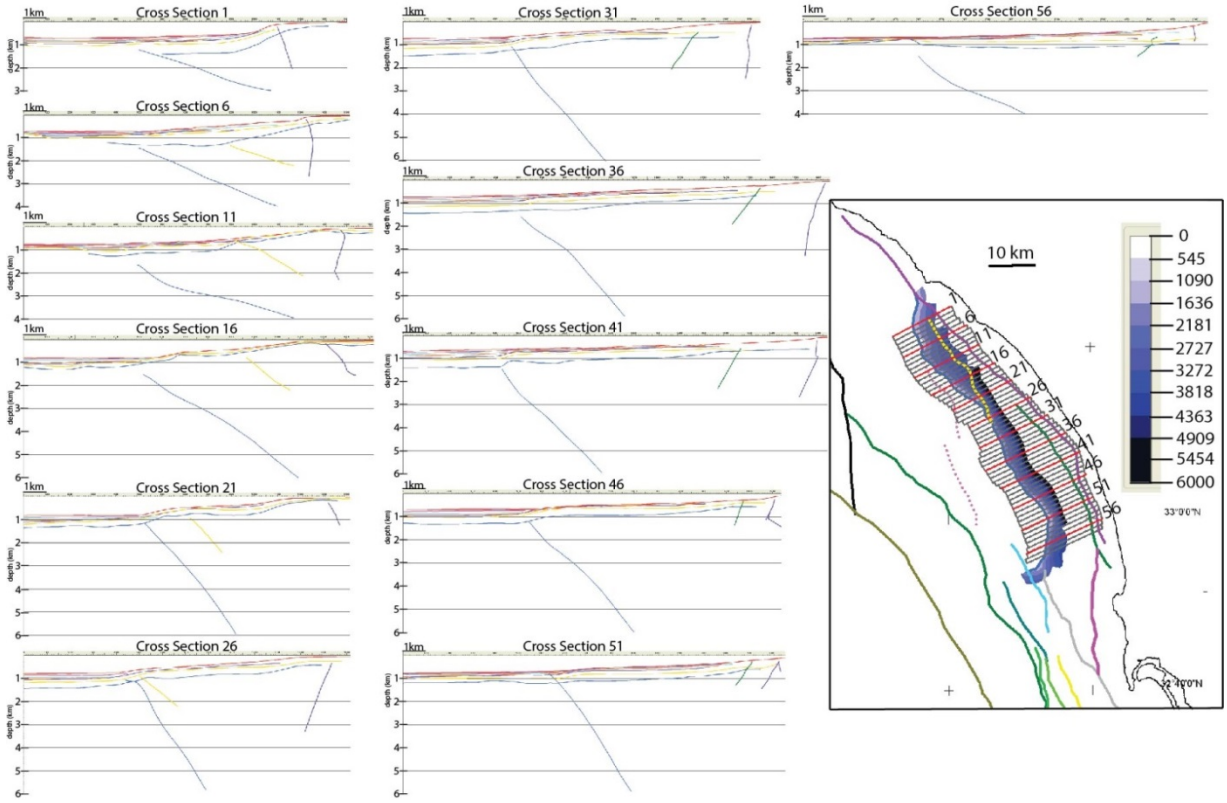

Figure 18:Every fifth cross section displayed from the 58 sections used for strike, dip, and structural relief measurements, displayed with no vertical exaggeration in depth. The San Mateo-Carlsbad fault is blue; Slope fault NW is yellow; Slope fault SE is dark green; and the Newport-Inglewood fault is violet. The map shows the depth-converted San Mateo-Carlsbad fault, as well as the locations for the 58 cross sections. These sections are spaced 1 km apart, with every fifth one displayed here indicated by a red line. Modified from *Bennett* [2012].

The paired plan and oblique views of the southern faults illustrate the 18 km right-stepover between the centers of the northern and southern flower structures (Figure 20). This distance is measured from the projected downdip intersections of the main oppositely-dipping faults. Both the Coronado Bank fault system and the Descanso fault consist of left-stepping en-echelon strands (Figure 20). There is Quaternary contraction across the northern faults, and Quaternary extension across the southern faults, as demonstrated by deformation of stratal horizons (Figures 13 through 19).

We interpret that the San Mateo-Carlsbad fault is continuous (Fig. 1), while publications map it as discontinuous [*Ryan et al*., 2009] or discontinuous and incomplete [*Jennings et al.,* 2010]. In contrast, we interpret the Oceanside thrust of *Rivero et al* [2000] or *Rivero and Shaw* [2011] to be comprised of discontinuous strands (Thin violet curves labeled "OT" on Fig. 1). The continuity of our San Mateo-Carlsbad fault compared to the discontinuous San Mateo, Oceanside, and Carlsbad separate faults of *Ryan et al.* [2009] is likely related to different mapping strategies, and is not actually a disagreement. *Ryan et al.* [2009] mapped the discontinuous/complex shallow strands above our underlying partly blind fault.

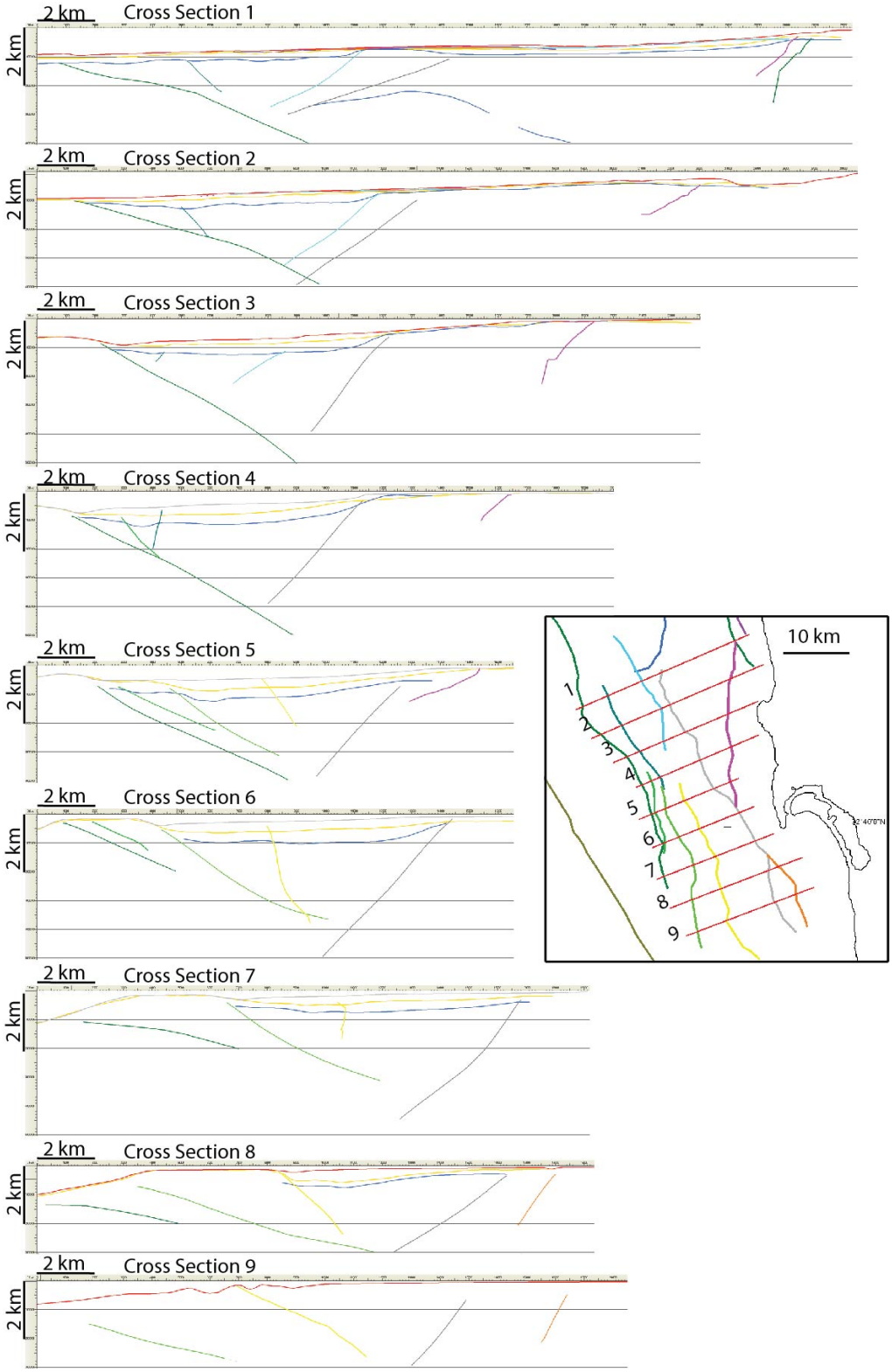

Figure 19: Cross sections with no vertical exaggeration across faults located south of the major right step over, offshore San Diego. Fault colors on the map correspond to colors on the cross sections. Horizons are sea floor (Red), top Lower Pico (Yellow), and H4 (blue). From *Bennett* [2012].

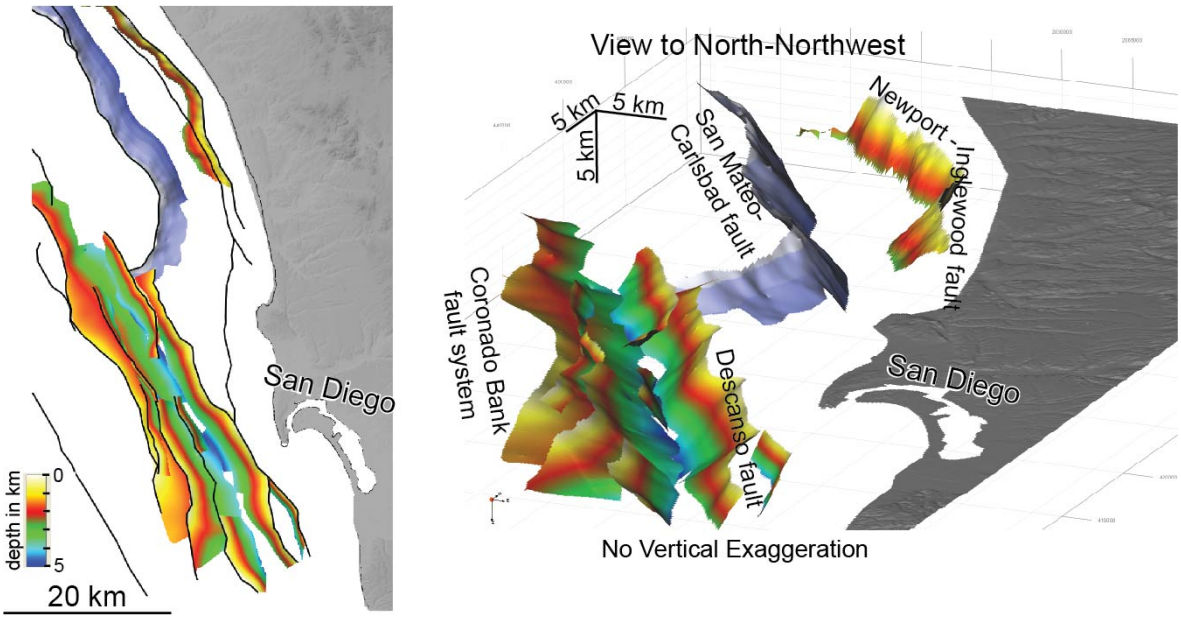

Figure 20: Right: An oblique view to the North-northwest of depth-converted fault surfaces, displayed with no vertical exaggeration. This perspective illustrates the major right step-over between the northern and southern flower structures. The southern faults display a left-stepping en-echelon pattern. Left: The same volume, displaying faults in plan-view. Those displayed as upper traces only were too steep to grid and then depth convert using the 3D velocity model, given the approach we were using in the Kingdom Suite software. They were depth-converted using single time-depth charts constructed using the Harvard version of the SCEC Community velocity model. Refer to Figures 18 and 19 for the geometry of these steep faults in cross section, together with the gridded faults. Some of the faults continue beyond where they were mapped, especially in the south at the offshore Mexican border, and the Newport-Inglewood fault as it comes onshore as the Rose Canyon fault. Figure modified from *Bennett* [2012].

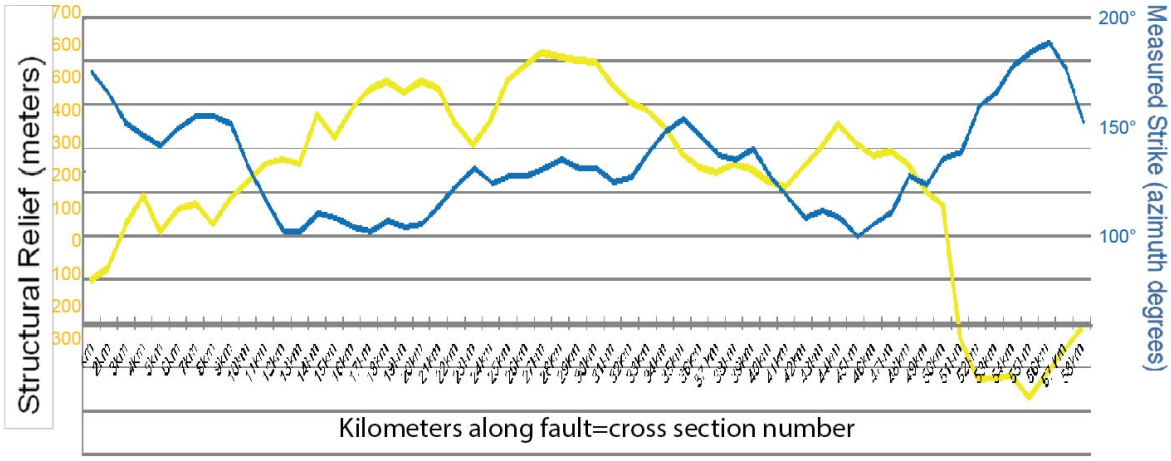

Figure 21: A line graph illustrating the relationship between San Mateo-Carlsbad (SMC) smoothed strike in azimuth degrees (Blue) and measured Top Lower Pico (TLP) structural relief (yellow). Positive (reverse separation) TLP relief is measured between km 3 and 50. TLP relief becomes negative (normal separation) after km 51. More E-W strikes are associated with the largest contractional relief, while more N-S strikes are associated with extensional structural relief. Modified from *Bennett* [2012].

3.2: Displacement Modeling.

Figure 21 demonstrates that reverse structural relief is highest across parts of the San Mateo-Carlsbad fault that strike more E-W, and are smallest, or normal, on parts that strike more N-S. The results of the trigonometric displacement modeling explained in Section 2 are displayed in Figures 22 to 24 and explained in their captions. The end result of these graphs is that thrust/reverse slip does not explain the vertical component of deformation due to faulting an folding (structural relief of ~1.95 Ma top Lower Pico). The deformation along the southern part of the fault is consistent with right-lateral strike-slip, and with right-lateral slip with a small reverse component along the central fault. Less than 1 km of displacement can produce the deformation of the top Lower Pico, so average slip rates have been less than 0.5 mm/yr. Relief by folding above a blind fault can be greater than the vertical component of slip on the fault. This is related to development of a forelimb. Since there is a forelimb above much of the fault (Figs. 14, 18), our results may overestimate displacement on parts of the fault. In the far north, for example cross sections 1-6, hanging-wall tilting extends farther ENE than the 4 km limit for measurement, and so the fault is blind here and total relief under-estimated (Fig. 18).

Structural relief of the top Lower Pico, Q4 (~600 ka), and Q3 (300-450 ka) was plotted against fault strike along 25 km of the fault (Fig. 25). A similar relief pattern suggests that the same type of deformation occurred after 450 ka. Some of the vertical relief of Q4 and Q3 could be due to initial vertical position at the time of deposition (sea floor relief). However, there are locations where thinning near the Q4 (violet) horizon across anticlines did not initiate until the time of that deposition. We interpret that to be related to a slight change in slip direction from near pure strike-slip to transpression. The fault was active before Q4 deposition, but, at least locally, the rate of increase of structural relief may have increased after deposition of Q4.

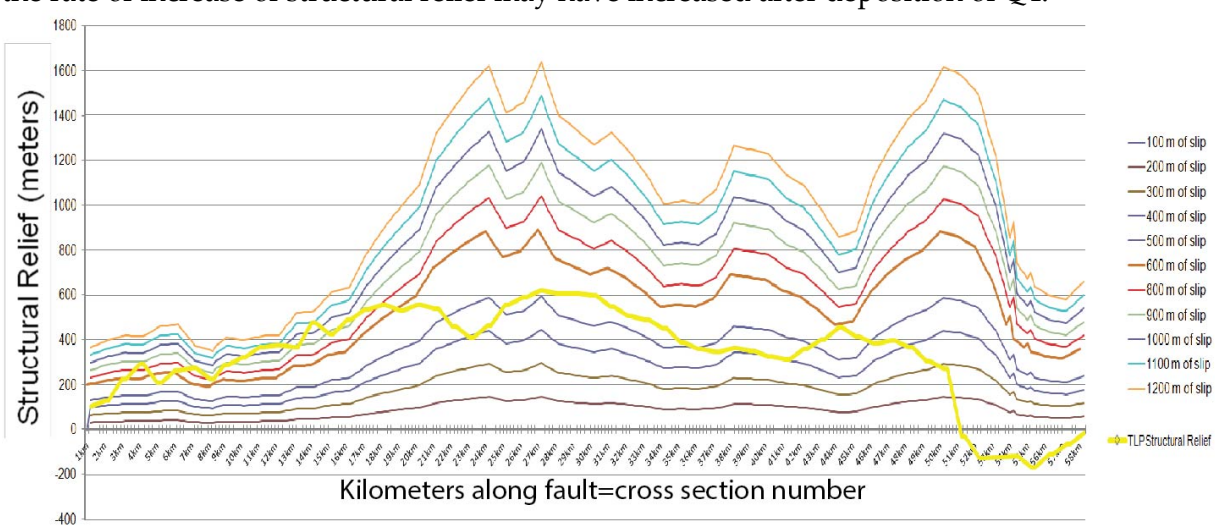

Figure 22: A line graph comparing modeled to measured (yellow) structural relief for top Lower Pico for a series of different displacements. Top Lower Pico is 1.95 Ma +/- 0.15 Ma in parts of the Los Angeles region [*Blake*, 1991]. The slip vector modeled here has the hanging-wall move towards an azimuth of 242° relative to the footwall. This motion is perpendicular to the average strike of the northern 50 km of this part of the fault, or nearly pure reverse slip. The match between modeled and measured structural relief is poor in the south (negative relief cannot be modeled) and not very good in the central section either. Modified from *Bennett* [2012].

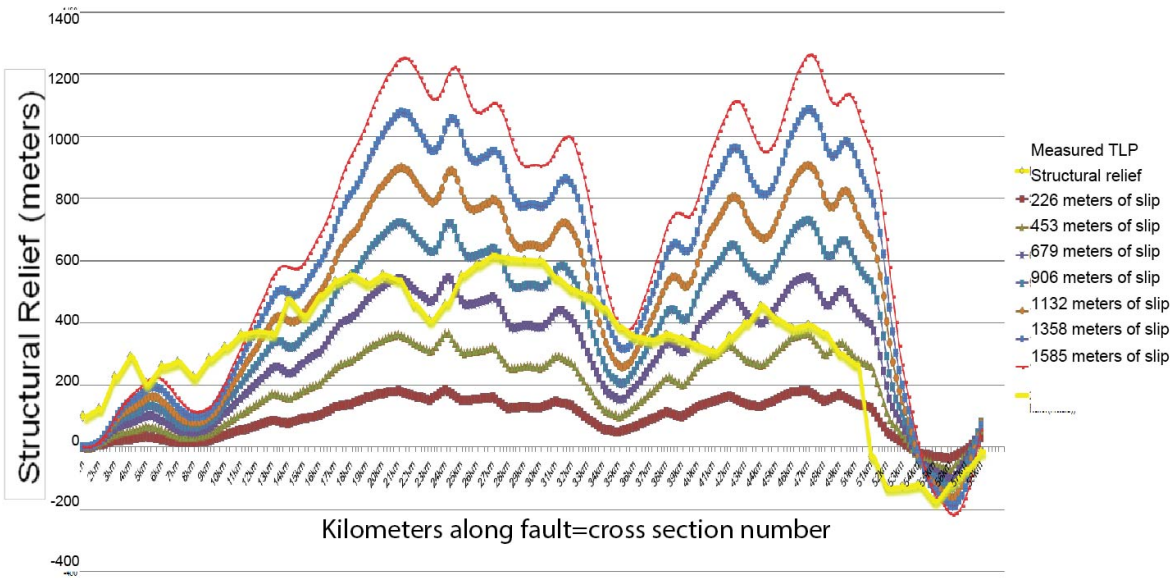

Figure 23: A line graph comparing an azimuth 162˚ motion of the hanging wall block with respect to the footwall block and measured top Lower Pico structural relief. The effects of second-order bends in fault strike (Fig. 21) are reflected in the double peak of the modeled and measured structural relief towards the middle of this graph. The match between modeled and measured structural relief is good in the central and southern parts of this fault, the San Mateo-Carlsbad fault, for displacements of between 679 m and 906 m in the south. This modeled displacement can be an overestimate in places where the fault is blind, depending on the fold model. Modified from *Bennett* [2012].

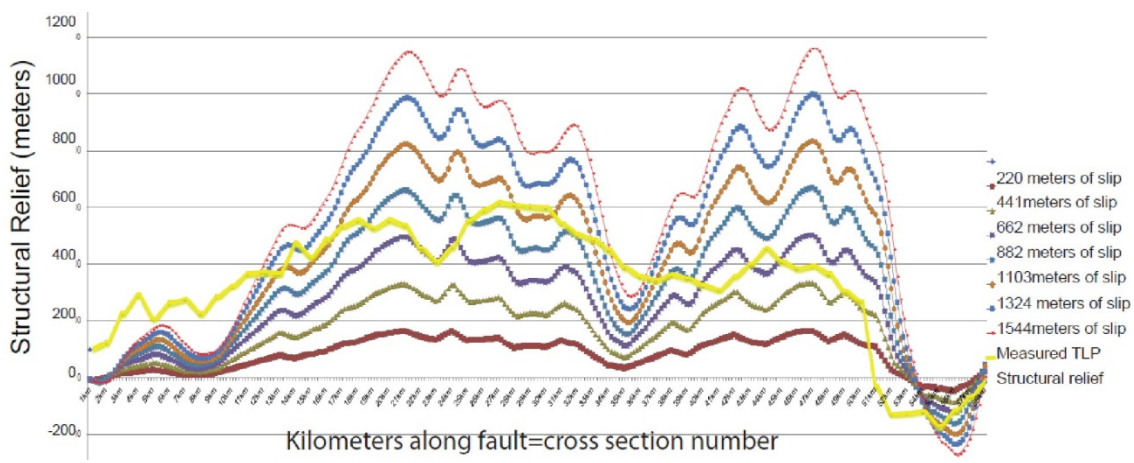

Figure 24: Graph comparing an azimuth 177˚ motion of the hanging wall block with respect to the footwall block and measured top Lower Pico structural relief. The match between modeled and measured structural relief is good in the central and southern parts of this fault, the San Mateo-Carlsbad fault, for displacements of between 662 m and 882 m in the south. The effects of second-order bends in fault strike (Figure 21) are reflected in the double peak of the modeled and measured structural relief towards the middle of this graph. The match is perhaps a little better than the 162˚ displacement azimuth in the south and a little worse in the central and northern parts. This modeled displacement can be an overestimate in places where the fault is blind, depending on the fold model. The northern part of the fault may be best modeled with right-reverse oblique displacement. Modified from *Bennett* [2012].

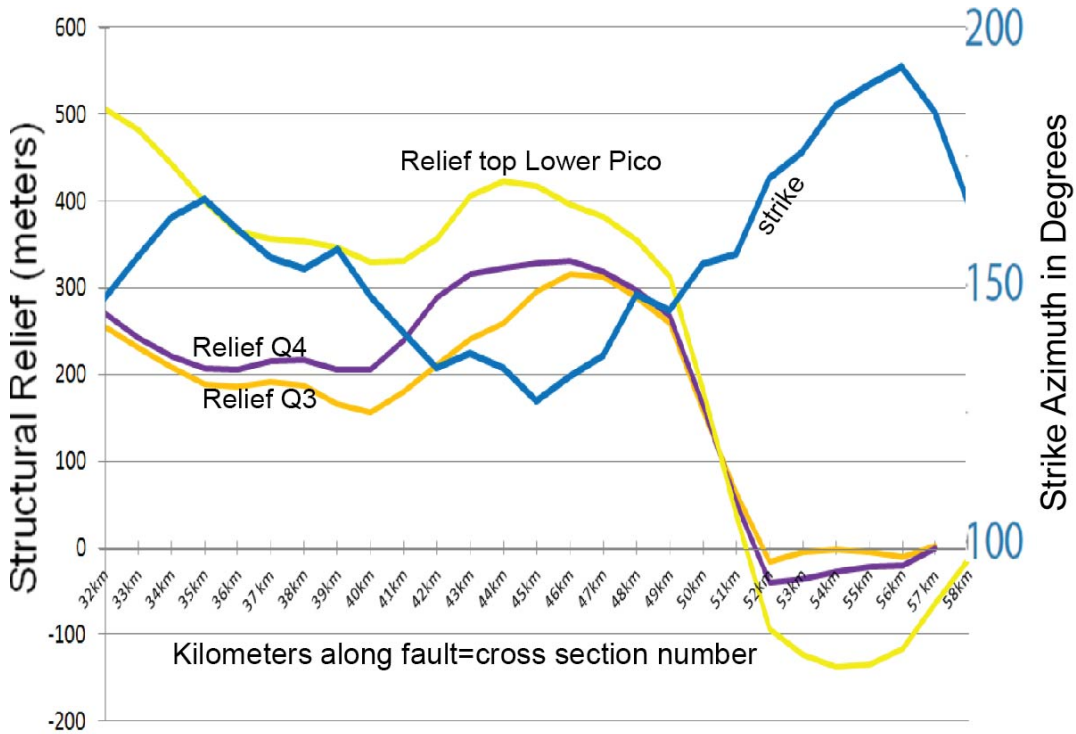

Figure 25: A line graph with smoothed (running average) values, comparing measured Q3 (orange), Q4 (violet) and top Lower Pico TLP (yellow) vertical deformation against the strike (blue) of the San Mateo-Carlsbad fault. The fault strike azimuth is displayed in blue. This graph shows measurements between km 32 and km 57, where Top Lower Pico, Q4, and Q3 could be interpreted on both sides of the fault. Measured structural relief for these horizons is progressively less for younger horizons, as expected for a fault active during sedimentation. The relief pattern is similar, suggesting the post-1.95 Ma average displacement direction continued at least to the <450 ka age of Q3 (orange). Modified from *Bennett* [2012].

3.3: Quaternary Sedimentation

Isochore (vertical thickness) maps, shown in Figure 26, were produced from the depth-converted top Lower Pico, Q4 through Q1 sequence boundaries, and the seafloor. These maps illustrate that sediment accumulation was localized and changed position through time. Thick areas coincide with the locations of submarine fans interpreted by *Covault and Romans* [2009]. We interpret the base of the submarine fans to be about 1.95 Ma, while *Covault and Romans* [2009] interpreted the fans to be 165 ka and younger (Fig. 8). Major onlap onto top Lower Pico (Fig. 12) and onto the Q horizons, especially Q4 (Fig. 5), represent missing section and thus missing time. Thus, a sequence boundary can represent much more time than one glacial cycle in the Inner Continental Borderland, especially on the paleo-Continental Slope. For example, a scientific corehole in Long Beach Harbor sampled post-780 ka strata above an unconformity and pre-2 Ma strata below it (Figs. 5, 7)[*Ponti et al.*, 2007; *Edwards et al.*, 2009].

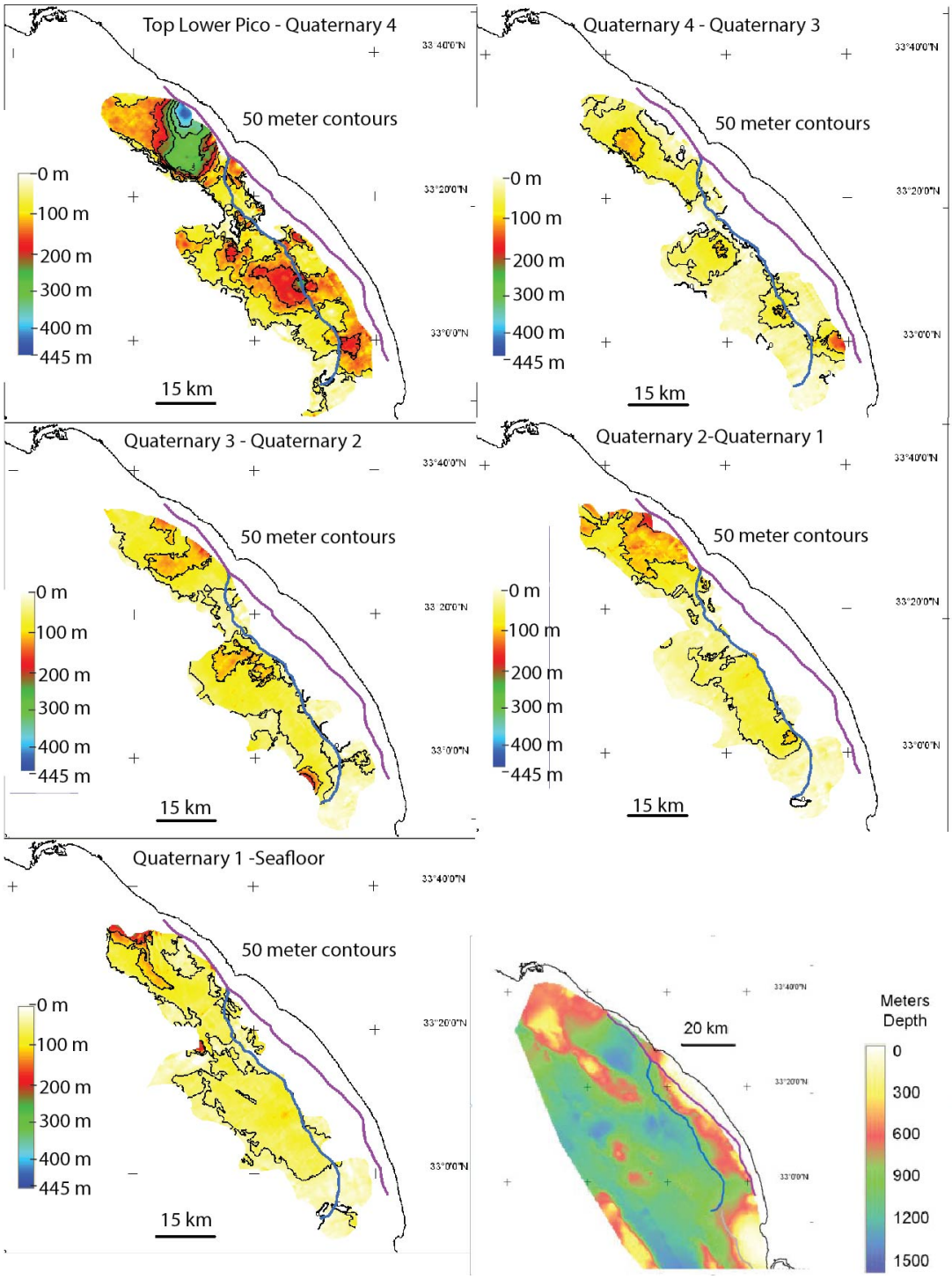

Figure 26: Isochore (vertical thickness) maps constructed from the interpreted Quaternary horizons. The map at the lower right is the top Lower Pico. The others maps display thicknesses between stratigraphic horizons labeled at the top of each one. Depocenters greatly shifted with time, so that there may be much missing section at any one location. Age models that relied on seismic stratigraphy and the late Quaternary dated 100 ka glacial cycles would underestimate stratal ages if a sequence boundary represents a long hiatus. Upper edge traces of the San Mateo-Carlsbad (blue) and Newport-Inglewood (violet) are displayed. Modified from *Bennett* [2012].

4: **Discussion and Conclusions**

4.1: Geometry

The products from this study detailed in the previous sections include: new depth-converted 3D representations of fault strands, kinematic and geometric evidence supporting a San Mateo-Carlsbad fault that is continuous for at least 58 km, and new age constraints on Quaternary sedimentation and thus deformation timing and rates. Oppositely-dipping fault strands intersect at depth, forming asymmetric (north) and symmetric (south) flower structure geometries. We document that faults published as thrusts are strike-slip (Carlsbad "thrust"), are not active during Quaternary time, preserving normal separation (central Oceanside "thrust")[*Campbell et al.*, 2009], and question whether the low-angle 30 Mile Bank fault, a Miocene oblique-normal fault, has been more than locally reactivated as a thrust.

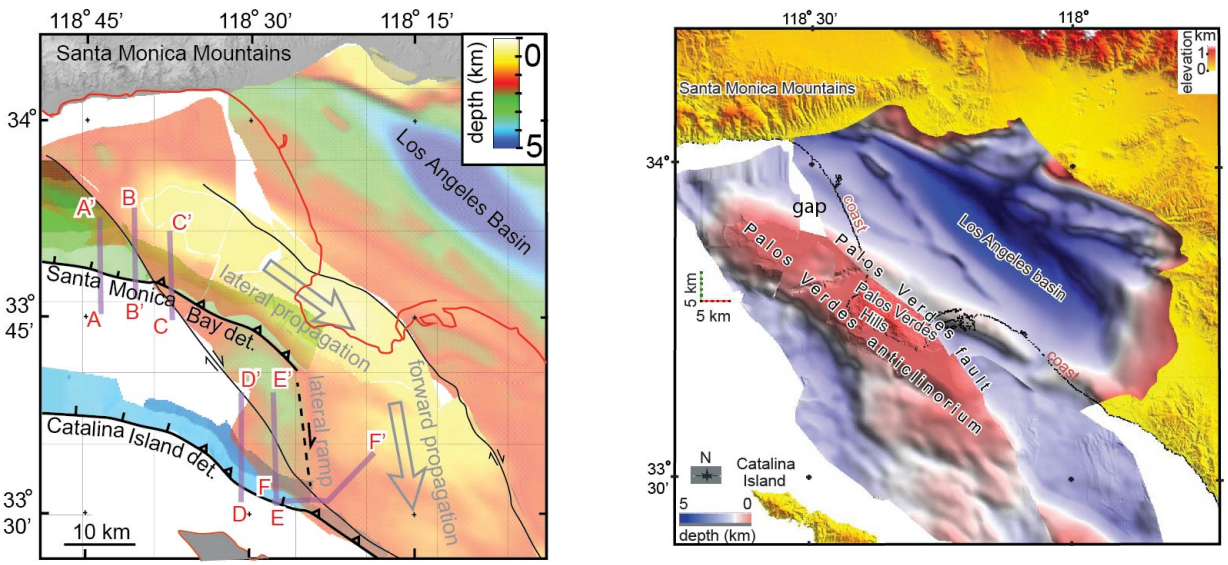

Figure 27 Left: Plan view of the semi-transparent near base Repetto (~4.5 Ma) horizon; Miocene/post-Miocene unconformity in the northwest. The Catalina Island detachment and Santa Monica Bay detachment are displayed respectively in blues and greens with the tone changing at even kilometer depths. Gray arrows and labels indicate our proposed southeast lateral propagation, and south forward propagation east of a blind lateral ramp (or tear fault). Black tics on fault hanging-walls indicate that Miocene normal component of slip is preserved; while triangles indicate significant thrust reactivation as Palos Verdes anticlinorium overrides the low-angle faults. The seismic reflection profiles displayed in Figure 9 are located. The northeast part, including Los Angeles Basin, was digitized from *Wright* [1991]. NW-striking right-lateral faults displayed at left as thin black curves are the San Pedro Basin fault (west) and Palos Verdes fault (east). **Right:** More regional opaque plan view of the same horizons. The Palos Verdes anticlinorium is a huge structure that can only partly be explained by oblique slip on the Palos Verdes fault. Both parts from *Sorlien et al.* [2013].

An ~18 km right stepover between a northern transpressional flower structure and a southern transtensional flower structure near 33° N marks a ENE-WSW limit between Quaternary transpression (north) and transtension (south) that includes San Diego Trough above the 30

Mile Bank fault (Fig. 1). There is no evidence for Quaternary shortening south of that line, at least at the resolution of the industry seismic reflection data.

4.2: San Mateo-Carlsbad Kinematics and Slip Rate

Simple geometrical modeling is applied to predict the vertical deformation that would result across the San Mateo-Carlsbad fault for a range of slip direction and range of cumulative slip. Its average slip rate since deposition of 1.95 Ma top Lower Pico is 0.5 mm/yr or less, and the slip is right-lateral in its southern and central parts. In contrast, *Covault and Romans*' [2009] assigned strata above our top Lower Pico horizon to Oxygen isotopic stage 6, 165 ka and younger. Such a young age model would produce slip estimates in excess of 5 mm/yr for the San Mateo-Carlsbad fault.

One can imply that the <0.5 mm/yr of right-lateral slip on the San Mateo-Carlsbad would continue onto the Descanso-Coronado Bank flower structure. Additional right-lateral slip could be linked to this fault system from the Palos Verdes fault to the north [*Legg*, 1991], and from a fault we mapped that connect the Newport Inglewood and Descanso faults (Fig. 1). However, we have not been able to directly model displacement on the southern faults, so any slip rate and direction we could provide would be too speculative. An integrated high-resolution seismic reflection and coring study would seem valuable, given proximity to San Diego.

4.3: The Palos Verdes anticlinorium folding above (oblique) thrust-reactivated Miocene low-angle normal faults.

Figure 27 presents the geometry of a 4.5-5 Ma horizon, as well as a model for its folding above the newly-interpreted Catalina Island detachment and re-interpreted Santa Monica Bay detachment (also Fig. 1). The Palos Verdes anticlinorium is 70 km-long and there is a 700 m-high seafloor fold scarp above its southwest limb (Fig. 2). Large-displacement low-angle (oblique) normal faults exposing blue schist in their footwalls would logically not be cut off by later strike-slip faults, and these faults should exist beneath Los Angeles basin [also *Davis et al.*, 1989; *Shaw and Suppe*, 1996]. Such surfaces would be available for reactivation during Plio-Quaternary shortening. Rates of thrust slip that may exceed 1 mm/yr could be produce rare major earthquakes [*Sorlien et al.*, 2013].

Elsewhere, shallow thrust reactivation of the >200 km-long series of low-angle normal faults seems to be localized near sea floor knolls, and may be associated with bends in local strike-slip faults, especially the San Pedro Basin fault. And, as discussed above, there is little or no evidence of thrust reactivation south of a WSW-ENE line through the northern bend of the San Mateo-Carlsbad fault.

5.0: Data availability

All seismic reflection data are available from the USGS NAMSS web site (Hart and Childs, 2005). The bathymetry data are also publicly available as described in the text. Nine of the depth-converted fault surfaces were provided to Craig Nicholson and Andreas Plesch and incorporated by them to the SCEC Community Model. Several other fault interpretations are being prepared for Nicholson and Plesch. The stratigraphic interpretation in the north is a supplement to Sorlien et al. [2013]. Some part of this report will be modified for publication, at which time the southern stratigraphic interpretation will be included as a supplement.

6.0: Acknowledgments: Funded by USGS-NEHRP G12AP20069. We acknowledge the support of Paradigm for the discounted use of Gocad and IHS for the donation of The Kingdom Suite Software. The authors acknowledge WesternGeco, Chevron, and the U.S. Geological Survey for providing the seismic reflection data for the purpose of this research. Background geologic discussions with Mark Legg, R. "Dan" Francis, and Craig Nicholson are appreciated. Brian Campbell and Billy Alward did much work loading the seismic reflection data and in interpretation; Robert Bauer was an academic advisor for the Bennett thesis and was involved in discussions.

7.0 References

Alward, W. S., C. C. Sorlien, R. L. Bauer, and B. A. Campbell (2009), Mergence of the Palos Verdes, San Pedro Basin, and San Diego Trough fault zones: A 220+ km-long fault system, Southern California Earthquake Center Annual Meeting, Proceedings and Abstracts v. XIX poster 2-024, p. 263.

Atwater, T., and J. M. Stock (1998), Pacific-North America plate tectonics of the Neogene southwestern United States: An update, *Int. Geol. Rev.*, 40, 375–402, doi:10.1080/00206819809465216.

Bennett, J. T. (2012), Analysis of Quaternary faults and associated deformation of sedimentary basin fill: Inner Continental Borderland of Southern California, M.S. Thesis, University of Missouri. https://mospace.umsystem.edu/xmlui/bitstream/handle/10355/15935/Research.pdf?sequence=2

Blake, G. H., (1991), Review of the Neogene biostratigraphy and stratigraphy of the Los Angeles Basin and implications for basin evolution, in Active Margin Basins, *Am. Assoc. Petrol. Geol. Mem.* 52, edited by K. T. Biddle, pp. 135–184, AAPG, Tulsa, OK.

Bohannon, R. G., and E. L. Geist (1998), Upper crustal structure and Neogene tectonic development of the California Continental Borderland, *Geol. Soc. Am. Bull.*, 110, 779–800, doi:10.1130/0016-7606.

Brankman, C. M., and J. H. Shaw (2009), Structural geometry andslip of the Palos Verdes fault, southern California: Implications for earthquake hazards, *Bull. Seismol. Soc. Am.*, 99, 1730–1745, doi:10.1130/0016-7606(1998)110<0779:UCSANT>2.3.CO;2.

California Division Oil, Gas, and Geothermal Resources (1992), California Oil & Gas Fields, Volume II: Southern, Central Coastal, and Offshore California, Pub. TR11.

Campbell, B. A., C. C. Sorlien, M.-H. Cormier, and W. S. Alward, 2009, Quaternary deformation related to the 3D geometry of the Carlsbad fault, offshore San Clemente to San Diego, Southern California Earthquake Center Annual Meeting, Proceedings and Abstracts v. XIX poster 2-025, p. 263-264.

Covault, J. A., and B. W. Romans (2009), Growth patterns of deep-sea fans revisited: Turbidite-system morphology in confined basins, examples from the California Borderland: *Marine Geology*, 265, p. 51-66.

Crouch, J. K., and J. Suppe (1993), Late Cenozoic tectonic evolution of the Los Angeles basin and inner California borderland: A model for core complex-like crustal extension, *Geol. Soc. Am. Bull.*, 105, 1415–1434, doi:10.1130/0016-7606(1993)105<1415:LCTEOT>2.3.CO;2.

Crowell, J. C. (1979), The San Andreas fault system through time, *J. Geol. Soc. Lond.*, 136, 293–302, doi:10.1144/gsjgs.136.3.0293.

Dartnell, P., and J. V. Gardner (1999), Sea-floor images and data from multibeam surveys in San Francisco Bay, Southern California, Hawaii, the Gulf of Mexico, and Lake Tahoe, California-Nevada, *U.S. Geol. Surv. Digital Data Series* DDS-55 Version 1.0.

Davis, T. L., J. Namson, and R. F. Yerkes (1989), A crosssection of the Los Angeles area: Seismically active fold and thrust belt, the 1987 Whittier Narrows earthquake, and earthquake hazard, *J. Geophys. Res.*, 94, 9644–9664, doi:10.1029/JB094iB07p09644.

Edwards, B. D., K. D. Ehman, D. J. Ponti, E. G. Reichard, J. C. Tinsley, R. J. Rosenbauer, and M. Land (2009), Stratigraphic controls on saltwater intrusion in the Dominguez Gap area in coastal Los Angeles, in Earth Science in the Urban Ocean: The Southern California Continental Borderland: *Geol. Soc. Am. Spec. Paper* 454, edited by H. J. Lee, and W. R. Normark, pp. 375–395, doi:10.1130/2009.2454(5.4).

Ehman, K. D., and B. D. Edwards (2013), Sequence stratigraphic framework of upper Pliocene to Holocene sediments of the Los Angeles basin, California: Implications for aquifer architecture, Book 112, Studies on Pacific Region Stratigraphy, edited by M. V. Caputo, Pacific Section SEPM (Society for Sedimentary Geology), Upland, CA, 49 pp.

Fisher, M. A., W. R. Normark, V. E. Langenheim, A. J. Calvert, and R. W. Sliter (2004), The offshore Palos Verdes fault zone near San Pedro, southern California, *Bull. Seismol. Soc. Am.*, 94, 1955–1983, doi:10.1785/0120030042.

Fuis, G. S., D. S. Scheirer, V, E, Langenheim, and M. D. Kohler (2012), A new perspective on the geometry of the San Andreas fault in southern California and its relationship to lithospheric structure, Bull. Seis. Soc. Amer., 102, 236-251, doi:10.1785/0120110041.

Hart, P. E. and J. R. Childs, 2005, National archive of marine seismic surveys (NAMSS): Status report on U. S. Geological Survey program providing access to proprietary data, Eos Trans. AGU, 86(18), Jt. Assem. Suppl., Abstract S41A-10, http://walrus.wr.usgs.gov/NAMSS/

Hill, M. L., and T. W. Dibblee, Jr. (1953), San Andreas, Garlock, and Big Pine faults, California: A study of the character, history, and tectonic significance of their displacements, Geol. Soc. Amer. Bull. 64, 443-458, doi: 10.1130/0016-7606(1953)64[443:SAGABP]2.0.CO;2

Jennings, C. W, W. A. Bryant, and G. Saucedo (2010), Fault activity map of California, California Geological Survey, Sacramento, California. http://www.consrv.ca.gov/cgs/cgs_history/PublishingImages/FAM_750k_MapRelease_page.jpg
http://www.quake.ca.gov/gmaps/FAM/faultactivitymap.html

Kamerling, M., and B. P. Luyendyk (1985), Paleomagnetism and Neogene tectonics of the northern Channel Islands, California, J. Geophys. Res., 90, p. 12485-12502.

Kansas Geological Survey (2001), Surface III, http://www.kgs.ku.edu/Tis/surf3/surf3Home.html.

Langenheim, V. E., R. C. Jachens, R. W. Graymer, J. P. Colgan, C. M. Wentworth, and R. G. Stanley (2012), Fault geometry and cumulative offsets in the central Coast Ranges, California: Evidence for northward increasing slip along the San Gergorio-San Simeon-Hosgri fault, *Lithosphere*, doi:10.1130/L233.1

Legg, M. R., (1991), Developments in understanding the tectonic evolution of the California Continental Borderland, in Osborne, R.H. ed., From shoreline to abyss: Contributions in marine geology in honor of Francis Parker Shepard: Tulsa, Oklahoma, *Soc. Economic Paleontol. and Mineral. Spec. Pub.* 46, p. 291–312.

Lisiecki, L. E., andM. E. Raymo (2005), A Pliocene–Pleistocene stack of 57 globally distributed benthic d18O records, *Paleoceanography*, 20, PA1003, doi:10.1029/2004PA001071.

Marlow, M. S., J. V. Gardner, and W. R. Normark (2000), Using high-resolution multibeam bathymetry to identify seafloor surface rupture along the Palos Verdes fault complex offshore southern California, *Geology*, 28, 587–590, doi:10.1130/0091-7613(2000)28<587:UHMBTI>2.0.CO;2.

McDougall, K., J. Hillhouse, C. Powell II, S. Mahan, E. Wan, and A. M. Sarna-Wojcicki (2012), Paleontology and geochronology of the Long Beach core sites and monitoring wells, Long Beach, California, *U.S. Geological Survey Open-File Report* 2011–1274, 235 pp., 18 plates. (http://pubs.usgs.gov/of/2011/1274/)

McNeilan, T. W., T. K. Rockwell, and G. S. Resnik (1996), Style and rate of Holocene slip, Palos Verdes Fault, Southern California, *J. Geophys. Res*., 101, 8317–8334, doi:10.1029/95JB02251.

Nardin, T. R., and T. L. Henyey (1978), Pliocene-Pleistocene diastrophism of Santa Monica and San Pedro shelves, California Continental Borderland, *Am. Assoc. Petrol. Geol. Bull.*, 62, 247–272.

Nicholson, C. (1996), Seismic behavior of the southern San Andreas fault zone in the northern Coachella Valley, California: Comparison of the 1948 and 1986 earthquake sequences, *Bull. Seism. Soc. Amer.*, 86, 1331-1349.

Nicholson, C., Sorlien, C. C., and Legg, M. R., 1993, Crustal imaging and extreme Miocene extension of the inner California Continental Borderland, Geological Society of America Abstracts With Programs, vol. 25, no. 6.

Nicholson, C., C. C. Sorlien, T. Atwater, J. C. Crowell, and B. P. Luyendyk (1994), Microplate capture, rotation of the Western Transverse Ranges, and initiation of the San Andreas transform as a low-angle fault system, *Geology*, 22, 491–495, doi:10.1130/0091-7613(1994)022<0491:MCROTW>2.3.CO;2.

Normark, W. R., D. J. W. Piper, and R. Sliter (2006), Sea-level and tectonic control of middle to late Pleistocene turbidite systems in Santa Monica Basin, offshore California, Sedimentology, 53, 867–897. doi:10.1111/j.1365-3091.2006.00797.x.

Normark, W. R., M. McGann, and R. W. Sliter, (2009), Late Quaternary sediment-accumulation rates within the inner basins of the California Continental Borderland in support of geologic hazard evaluation in Lee, H.J., and Normark, W.R., eds., Earth Science in the Urban Ocean: the Southern California Continental Borderland: *Geol. Soc. Amer. Spec. Paper* 454, 117-139.

Pinter, N., C. C. Sorlien, and A. T. Scott (2003), Fault-related fold growth and isostatic subsidence, California Channel Islands, *Am. J. Sci.*, 303, 300–318.

Plesch, A, J. H. Shaw, C. Benson, W. A. Bryant, S. Carena, M. Cooke, J. Dolan, G. Fuis, E. Gath, L. Grant, E. Hauksson, T. Jordan, M. Kamerling, M. Legg, S. Lindvall, H. Magistrale, C. Nicholson, N. Niemi, M. Oskin, S. Perry, G. Planansky, T. Rockwell, P. Shearer, C. Sorlien, M. P. Suss, J. Suppe, J. Treiman, and R. Yeats, Community Fault Model (CFM) for southern California, *Bull. Seismol. Soc. Am.*, 97, 1793–1802, doi:10.1785/0120050211.

Ponti, D.J., Ehman, K.D., Edwards, B.D., Tinsley, J.C., Hildenbrand, T., Hillhouse, J.W., Hanson, R.T., McDougall, K., Powell, C.L., Wan, E., Land, M. Mahan, S., Andrei, M., Sarna Wojcicki., 2007, A 3-Dimensional Model of Water-Bearing Sequences in the Dominguez Gap Region, Long Beach, California, *U.S. Geological Survey Open-File Report* 2007–1013, 34 pp., USGS, Reston, VA.

Rivero, C., J. H. Shaw, and K. Mueller (2000), Oceanside and Thirtymile Bank blind thrusts: Implications for earthquake hazards in coastal southern California: *Geology*, 28, p. 891-894.

Rivero, C., and J. H. Shaw, 2011, Active folding and blind thrust faulting induced by basin inversion processes, inner California borderlands, in K. McClay, J.H. Shaw, and J. Suppe, eds., Thrust Fault-Related Folding: *Amer. Assoc. Petrol. Geol. Memoir* 94, p. 187 – 214.

Roberts, A. P., (1995), Tectonic rotation about the termination of a major strike-slip fault, Marlborough fault system, New Zealand, Geophys. Res. Letters, 22, 187-190.

Ryan, H. F., M. R. Legg, J. E. Conrad, and R. W. Sliter, 2009, Recent faulting in the Gulf of Santa Catalina: San Diego to Dana Point, in H.J. Lee and W. R. Normark, eds., Earth Science in the Urban Ocean: The Southern California Continental Borderland: *Geol. Soc. Amer. Spec. Paper* 454, 291-315, doi: 10.1130/2009.2454(4.5).

Ryan, H. F., J. E. Conrad, C. K. Paull, and M. McGann (2012), Slip rate on the San Diego Trough fault zone, Inner California Borderland, and the 1986 Oceanside earthquake swarm revisited, *Bull. Seismol. Soc. Am.*, 102, 2300–2312, doi:10.1785/0120110317.

Seeber, L., and C. C. Sorlien (2000), Listric thrusts in the western Transverse Ranges, California, *Geol. Soc. Am. Bull.*, 112, 1067–1079, doi:10.1130/0016-7606(2000) 112<1067:LTITWT>2.0.CO;2.

Sengör, A. M. C., O. Tüysüz, C. İmren, M. Sakınç, H. Eyidoğan, N. Görür, X. Le Pichon, C. Rangin, (2005). The North Anatolian Fault: a new look. *Ann. Rev. Earth and Planet. Sciences* 33, 37–112. doi:10.1146/annurev.earth.32.101802.120415.

Shaw, J. H., and P.M. Shearer (1999), An elusive blind-thrust fault beneath metropolitan Los Angeles, *Science*, 283, 1516–1518, doi:10.1126/science.283.5407.1516.

Shaw, J. H., and J. Suppe (1996), Earthquake hazards of active blind-thrust faults under the central Los Angeles basin, California, *J. Geophys. Res.*, 101, 8623–8642, doi:10.2973/odp.proc.ir.167.109.1997.

Sliter, R. W., W. R. Normark, and C. E. Gutmacher (2005), Multichannel seismic-reflection data acquired off the coast of southern California-Part A 1997, 1998, 1999, and 2000, *U. S. Geological Survey Open-File Report 2005-1084*, http://pubs.usgs.gov/of/2005/1084/index.html.

Sliter, R. W., H. F. Ryan, and P. J. Triezenberg (2010), High-resolution seismic reflection data offshore Dana Point, Southern California Borderland, *U. S. Geological Survey Open-File Report* 2010-1111, http://pubs.usgs.gov/of/2010/1111/.

Sorlien, C. C., B. A. Campbell, and L. Seeber (2010), Geometry, kinematics, and activity of a young mainland-dipping fold and thrust belt: Newport Beach to San Clemente, California, Final Report to U.S. Geological Survey NEHRP, contract USDI/USGS 08HQGR0103, 25 pages, http://earthquake.usgs.gov/research/external/reports/08HQGR0103.pdf

Sorlien, C. C., M. J. Kamerling, L. Seeber, and K. G. Broderick (2006), Restraining segments and reactivation of the Santa Monica–Dume–Malibu Coast fault system, offshore Los Angeles, California, *J. Geophys. Res.*, 111. doi:10.1029/2005JB003632.

Sorlien, C . C., S. D. Akhun, L. Seeber, M. Steckler, D. Shillington, H. Kurt, G. Çifçi, D. T. Poyraz, S. Gürçay, D. Dondurur, C. İmren, E. Perincek, M. Kucuk, J. B. Diebold, 2012, Uniform basin growth over the last 500 ka, North Anatolian Fault, Marmara Sea, Turkey, *Tectonophysics*, doi:10.1016/j.tecto.2011.10.006.

Sorlien, C. C., L. Seeber, K. G. Broderick, B. P. Luyendyk, M. A. Fisher, R. W. Sliter, and W. R. Normark (2013), The Palos Verdes Anticlinorium along the Los Angeles, California coast: Implications for underlying thrust faulting, Geochem., Geophys., Geosyst.. http://onlinelibrary.wiley.com/doi/10.1002/ggge.20112/pdf DOI: 10.1002/ggge.20112

Suss, M. P., and J. H. Shaw (2003), P-wave seismic velocity structure derived from sonic logs and industry reflection data in the Los Angeles basin, California, J. Geophys. Res.,108, DOI: 10.1029/2001JB001628.

Sylvester, A.G., (1988), Strike-slip faults, Geol. Soc. Amer. Bull., 100, p.1666-1703.

Wilson, D. S., P. A. McCrory, and R. G. Stanley (2005), Implications of volcanism in coastal California for the Neogene deformation history of western North America, *Tectonics*, 24(3), TC3008, doi:10.1029/2003TC001621.

Wright, T. L. (1991), Structural geology and tectonic evolution of the Los Angeles Basin, California, in Active Margin Basins, *Am. Assoc. Petrol. Geol. Mem*., 52, edited by K. T. Biddle, pp. 35–134, AAPG, Tulsa, OK.

Yeats, R. S., and J. M. Beall (1991), Stratigraphic controls of oil fields in the Los Angeles basin, A guide to migration history, in Active Margin Basins, *Am. Assoc. Petrol. Geol. Mem.* 52, edited by K. T. Biddle, pp. 221–235, AAPG, Tulsa, OK.

Yeats, R. S. (1973), Newport-Inglewood fault zone, California, Amer. Assoc. Petrol. Geol. Bull., 57, 117-135.

8.0: Bibliography:

Bennett, J. T. (2012), Analysis of Quaternary faults and associated deformation of sedimentary basin fill: Inner Continental Borderland of Southern California, M.S. Thesis, University of Missouri. https://mospace.umsystem.edu/xmlui/bitstream/handle/10355/15935/Research.pdf?sequence=2

Sorlien, C. C., L. Seeber, K. G. Broderick, B. P. Luyendyk, M. A. Fisher, R. W. Sliter, and W. R. Normark (2013), The Palos Verdes Anticlinorium along the Los Angeles, California coast: Implications for underlying thrust faulting, Geochem., Geophys., Geosyst.. http://onlinelibrary.wiley.com/doi/10.1002/ggge.20112/pdf DOI: 10.1002/ggge.20112